Finding NHIM using LD: N-DoF quadratic normal form

Introduction

Identifying invariant manifolds in high dimensional phase space and their anchor, normally hyperbolic invariant manifold (NHIM), is the stepping stone in applying phase space transport methods to a broad array of problems in physics, chemistry, and engineering (Wiggins 1990; Gottwald, Virgin, and Dowell 1995; Jaffé, Farrelly, and Uzer 1999; Oliveira et al. 2002; Dellnitz et al. 2005; Gabern et al. 2005; Gabern et al. 2006; Waalkens, Schubert, and Wiggins 2008; Waalkens and Wiggins 2010; Wiggins 2013; Wiggins 2016). These problems are typically formulated in phase space of more than 4 dimensions (that is, $N = 2$ or more degrees of freedom) and the geometric approach of computing invariant manifolds that are codimension-1 separatrices requires Poincaré-Birkoff normal form theory. The Poincaré-Birkoff normal form approach for computing NHIMs and their stable and unstable manifolds has only been developed for Hamiltonian systems in the neighborhood of index-k saddle points. This approach in itself is successful and rigorous, but its implementation requires experience in writing or using algebraic manipulation programs. Furthermore, these computations become expensive as the dimensions increase since Poincaré-Birkoff normal form theory is based on Taylor expansion, a high dimensional vector valued polynomial, of the Hamiltonian in a neighborhood of the saddle point to sufficiently high order. Besides, the resulting visualization can be non-obvious leading to cumbersome interpretation and can not work for high dimensions. The succcess and shortcoming of the vizualization approach based on topological methods for four-dimensional space becomes apparent when trying to extend the results in Refs. (Koçak et al. 1986; Banks 1992; Hoffmann and Zhou 1991). This raises the question of detecting the signatures of the high dimensional structures, if they exist, when probed with low dimensional surfaces. If one does manage to detect these structures, how do they manifest on the low dimensional surfaces.

One such method is the Lagrangian descriptors (LDs) developed in Refs. (Madrid and Mancho 2009; Mendoza and Mancho 2010; Mancho et al. 2013; Lopesino et al. 2017). Lagrangian descriptors are a class of trajectory diagnostic methods that can reveal phase space structures by encoding geometric property of trajectories (such as, phase space arc length, configuration space distance or displacement, cumulative action or kinetic energy) initialised on a two dimensional surface. The method was originally developed in the context of Lagrangian transport studies in fluid dynamics that requires identifying transport barriers which are the invariant manifolds in time dependent 2D fluid flow. Besides, the method applies to both Hamiltonian and non-Hamiltonian systems ((Lopesino et al. 2017)) as well as to systems with arbitrary, stochastic and dissipative, time-dependence ((Balibrea-Iniesta et al. 2016; Craven, Junginger, and Hernandez 2017; Junginger and Hernandez 2016a)). Lagrangian descriptor based detection of transport barriers has also been applied directly to data sets, such as those obtained from satellite observations or numerical simulations ((Cámara et al. 2012; Mendoza, Mancho, and Wiggins 2014; García-Garrido, Mancho, and Wiggins 2015; Ramos et al. 2018)). Furthermore, the method is straightforward to implement computationally and it provides a "high resolution" method for exploring the influence of high dimensional phase space structure on trajectory behaviour. The method of Lagrangian descriptors takes an [*opposite*]{} approach to that of Lyapunov exponent type calculations by emphasizing the initial conditions of trajectories, rather than their advected locations that is involved in calculating normalized rate of divergence. This is achieved by considering a two dimensional section of the full phase space and discretizing with a dense grid of initial conditions. Even though the trajectories wander off in the phase space, as the initial conditions evolve in time, there is no loss in resolution of the two dimensional section. Our objective is to clarify the use of Lagrangian descriptors as a diagnostic on two dimensional sections of high dimensional phase space structures. This diagnostic is also meant to be used as the preliminary step in computing the NHIM, their stable and unstable manifolds using other computational means (Junginger et al. 2016; Bardakcioglu et al. 2018; Ezra and Wiggins 2018). In this

article, we assess the capability of Lagrangian descriptors to detect the type of high dimensional phase space structures in Hamiltonian systems such as the NHIM, their stable, and unstable manifolds that are used in computing rates of chemical reactions.

Computing chemical reaction rates is based on the fundamental framework of transition state theory as formulated in phase space by Polanyi, Evans, Wigner, Eyring (Evans and Polanyi 1935; Wigner 1938; Eyring 1938; Garrett 2000)). Further research has shown that constructing a *locally* recrosssing free, minimal flux orientable surface called a [*dividing surface*]{} (DS) is the phase space structure that provides the correct estimate for reaction rates. This dividing surface of geometry $\mathbb{S}^{2N-2}$ (a 2N-2 dimensional sphere) is constructed from the NHIM of geometry $\mathbb{S}^{2N-3}$ which forms the equator of the dividing surface, on a constant energy surface (Waalkens and Wiggins 2004; Waalkens, Schubert, and Wiggins 2008; Waalkens and Wiggins 2010; Wiggins 2016). Furthermore, the global dynamics of reactive and non-reactive trajectories is governed by the invariant (stable and unstable) manifolds, of the NHIM, are $\mathbb{S}^{2N-3} \times \mathbb{R}$, and thus act as codimension-1 separatrices on the energy surface. Thus, the NHIM acts as the anchor for the local dynamics via the dividing surface from reactants to products or vice-versa and for the global dynamics via the stable/unstable invariant manifolds. Thus, detecting and constructing the NHIM forms a fundamental step in obtaining quantitative results in reaction dynamics (Ezra, Waalkens, and Wiggins 2009; Ezra and Wiggins 2018). In the present study, we will focus on detecting and verifying these high dimensional phase space structures.

Recently the applicability of the Lagrangian descriptor based approach to time dependent problems with random and dissipative forcing in chemical reaction dynamics has been shown whereby the transition state trajectory is calculated using the extremal values in Lagrangian descriptor values; see Refs. (Craven and Hernandez 2015; Craven and Hernandez 2016; Craven, Junginger, and Hernandez 2017; Junginger and Hernandez 2016b; Junginger et al. 2016; Junginger, Duvenbeck, et al. 2017; Junginger, Main, et al. 2017; Feldmaier et al. 2017; Revuelta et al. 2017; Patra and Keshavamurthy 2018). The initial conditions for the transition state trajectory is identified by computing the extrema of the Lagrangian descriptor on a two dimensional domain. Comparing extremal and singular features in the Lagrangian descriptor plot with invariant manifolds in three dimensional vector fields, Ref. (García-Garrido et al. 2018) has also provided numerical evidence for detecting NHIM using the LD on two dimensional surfaces. The authors presented the comparison using a stacked version of a two dimensional linear saddle, the duffing oscillator, and a time-perturbed 3D geophysical model. This has the advantage that the NHIM and the invariant manifolds are known exactly or can be computed with other established methods. For the problems considered therein, the NHIM (a curve embedded in 3D) and its associated invariant manifolds (a 2D surface in 3D) can be visualized in the 3D space since the dimensionality of phase space structures is less than 3. We take this approach to the next logical step by applying this to benchmark problems of two and three degrees-of-freedom Hamiltonian system where the phase space structures are known exactly, that is they can be written as closed-form analytical expressions This article is outlined as follows. In Section

$$sec : theory$$

, we describe the method of Lagrangian descriptor used in this study and present an analytical result on identifying invariant manifolds using features in the Lagrangian descriptor. In Section

$$sec : normal\_form\_2dof$$

and

$$sec : normal\_form\_3dof$$

, we discuss the benchmark systems and present numerical evidence of our claim using isoenergetic two-dimensional surfaces. In Section

$$sec : summ$$

, we summarize our results on detecting invariant manifolds and discuss related future directions.

Method of Lagrangian Descriptor

The Lagrangian descriptor (LD) as presented in Ref.(Madrid and Mancho 2009) is the arc length of a trajectory calculated on a chosen initial time t_0 and measured for fixed forward and backward integration

time, τ. For continuous time dynamical systems, Ref.(Lopesino et al. 2017) gives an alternative definition of the LD which is useful for proving rigorous results and can be computed along with the trajectory. It provides a characterization of the notion of singular features of the LD that facilitates a proof for detecting invariant manifolds in certain model situations. In addition, the "additive nature" of this new definition of LD provides an approach for assessing the influence of each degree-of-freedom separately on the Lagrangian descriptor. This property was used in Ref.(Demian and Wiggins 2017) which showed that a Lagrangian descriptor can be used to detect Lyapunov periodic orbits in the two degrees-of-freedom H[é]{}non-Heiles Hamiltonian system. We will describe this procedure for two and three degrees-of-freedom linear autonomous Hamiltonian systems. We begin by establishing notation in the general setting of a time-dependent vector field where

$$\frac{d\mathbf{x}}{dt} = \mathbf{v}(\mathbf{x}, t), \quad \mathbf{x} \in \mathbb{R}^n , \ t \in \mathbb{R}$$

where $\mathbf{v}(\mathbf{x}, t) \in C^r$ $(r \geq 1)$ in $\mathbf{x}$ and continuous in time. The definition of LDs depends on the initial condition $\mathbf{x}_0 = \mathbf{x}(t_0)$, on the initial time t_0 (trivial for autonomous systems) and the integration time τ, and the type of norm of the trajectory's components, and takes the form,

$$M_p(\mathbf{x}_0, t_0, \tau) = \int_{t_0 - \tau}^{t_0 + \tau} \sum_{i=1}^{n} |\dot{x}_i(t; \mathbf{x}_0)|^p \ dt \tag{1}$$

where $p \in (0, 1]$ and $\tau \in \mathbb{R}^+$ are freely chosen parameters, and the overdot symbol represents the derivative with respect to time. It is to be noted here that there are three formulations of the function M_p in the literature: the arc length of a trajectory in phase space (Madrid and Mancho 2009), the arc length of a trajectory projected on the configuration space (Junginger et al. 2016; Junginger and Hernandez 2016b; Junginger, Duvenbeck, et al. 2017; Junginger, Main, et al. 2017), and the sum of the p-norm of the vector field components (Lopesino et al. 2015; Lopesino et al. 2017). Although the latter formulation of the Lagrangian descriptor developed in Ref. (Lopesino et al. 2015; Lopesino et al. 2017) does not resemble the arc length, the numerical results using either of these forms have been shown to be in agreement and promise of predictive capability in geophysical flows (Cámara et al. 2012; Mendoza, Mancho, and Wiggins 2014; García-Garrido, Mancho, and Wiggins 2015; Ramos et al. 2018). The formulation we adopt here is motivated by the fact that this allows for proving rigorous result, which we will discuss in the next section, connecting the singular features and minimum in the LD plots with NHIM and its stable and unstable manifolds. It follows from the result that

$$\mathcal{W}^s(\mathbf{x}_0, t_0) = \mathrm{argmin} \ \mathcal{L}^{(f)}(\mathbf{x}_0, t_0, \tau)$$
$$\mathcal{W}^u(\mathbf{x}_0, t_0) = \mathrm{argmin} \ \mathcal{L}^{(b)}(\mathbf{x}_0, t_0, \tau)$$

where the stable and unstable manifolds ($\mathcal{W}^s(\mathbf{x}_0, t_0)$ and $\mathcal{W}^u(\mathbf{x}_0, t_0)$) denote the invariant manifolds at intial time t_0 and argmin $(\cdot)$ denotes the argument that minimizes the function $\mathcal{L}^{(\cdot)}(\mathbf{x}_0, t_0, \tau)$ in forward and backward time, respectively. In addition, the coordinates of the NHIM at time t_0 is given by the intersection $\mathcal{W}^s(\mathbf{x}_0, t_0)$ and $\mathcal{W}^u(\mathbf{x}_0, t_0)$ of the stable and unstable manifolds, and thus given by

$$\mathcal{M}(\mathbf{x}_0, t_0) = \mathrm{argmin} \ \left(\mathcal{L}^{(f)}(\mathbf{x}_0, t_0, \tau) + \mathcal{L}^{(b)}(\mathbf{x}_0, t_0, \tau) \right) = \mathrm{argmin} \ \mathcal{L}(\mathbf{x}_0, t_0, \tau) \qquad \text{NHIM}$$

Two Degrees of Freedom

In this section we use the Lagrangian descriptor method to identify the NHIM and its stable and unstable manifolds for a 2 DoF separable quadratic Hamiltonian with an index-1 saddle at the origin. The advantage of using this model Hamiltonian is that we can compare the analytical expressions for the phase space structures with features in LD plots.

Decoupled quadratic Hamiltonian

We consider a quadratic Hamiltonian for a two degree-of-freedom system given by

$$H(q_1, p_1, q_2, p_2) = \underbrace{\frac{\lambda}{2}(p_1^2 - q_1^2)}_{H_r} + \underbrace{\frac{\omega_2}{2}(q_2^2 + p_2^2)}_{H_b}, \quad \lambda, \omega_2 > 0$$

with the corresponding vector field

$$\dot{q}_1 = \frac{\partial H_2}{\partial p_1} = \lambda p_1,$$

$$\dot{p}_1 = -\frac{\partial H_2}{\partial q_1} = \lambda q_1,$$

$$\dot{q}_2 = \frac{\partial H_2}{\partial p_2} = \omega_2 p_2,$$

$$\dot{p}_2 = -\frac{\partial H_2}{\partial q_2} = -\omega_2 q_2$$

The equilibirum point is located at $(0,0,0,0)$ on the zero total energy surface. It is trivial to check that the eigenvalues of the linearized system around the equilibrium point are $\pm\lambda$ and $\pm i\omega_2$, and hence the equilibrium point is of saddle $\times$ center type. In this form, the Hamiltonian is decoupled into the "reactive" mode given by H_r and the "bath" mode given by H_b, hence it will be referred to as separable quadratic Hamiltonian (SQH). This representation lends to discussing the distribution of total energy between the two modes for the phase space structures in uncoupled coordinates. In this form, a chemical reaction is said to have occurred when the q_1 coordinate of a trajectory changes sign and thus, an isoenergetic, $H(q_1, p_1, q_2, p_2) = h$, dividing surface (DS) can be defined by $q_1 = 0$ hypersurface. The constant energy defines a three dimensional surface in the four dimensional phase space and is given by

$$\frac{\lambda}{2}(p_1^2 - q_1^2) + \frac{\omega_2}{2}(p_2^2 + q_2^2) = H_r + H_b = h > 0, \qquad H_r > 0, \quad H_b \geq 0$$

The dividing surface, $q_1 = 0$, for a constant energy is

$$\frac{\lambda}{2}p_1^2 + \frac{\omega_2}{2}(p_2^2 + q_2^2) = H_r + H_b = h > 0, \qquad H_r > 0, \quad H_b \geq 0$$

which is a two dimensional surface, or precisely of geometry $\mathbb{S}^2$, that is a 2-sphere on the three dimensional energy surface. Thus it is codimension-1 and partitions the energy surface into reactant $p_1 - q_1 > 0$ and product $p_1 - q_1 < 0$ regions by the forward and backward "reaction" dividing surfaces as shown in Ref. (Waalkens and Wiggins 2004) and given by

$$p_1 = \pm\sqrt{\frac{2}{\lambda}\left(H_r + H_b - \frac{\omega_2}{2}(p_2^2 + q_2^2)\right)}, \quad \text{forward/backward DS}$$

The forward and backward DS is joined at $p_1 = 0$, thus

$$\mathcal{M}(h) = \left\{(q_1, p_1, q_2, p_2) \mid q_1 = 0, p_1 = 0, \frac{\omega_2}{2}(p_2^2 + q_2^2) = H_b = h \geq 0\right\} \qquad \text{NHIM}$$

which is of geometry $\mathbb{S}^1$, that is a circle centered at the origin and of radius $\sqrt{2h/\omega_2}$ in the (q_2, p_2) plane. This is a [*normally hyperbolic invariant manifold*]{} (NHIM) associated with the index-1 saddle and parametrized by total energy $H(q_1, p_1, q_2, p_2) = h$ (Wiggins 2013). [*Invariance*]{} follows from the vector field since when $q_1 = p_1 = 0$, $\dot{q}_1 = \dot{p}_1 = 0$. Thus q_1 and p_1 always remain zero, and trajectories with these initial conditions remain on the NHIM, that is, $q_1 = p_1 = 0$ is invariant. It is [*normally hyperbolic*]{} since the directions normal to the NHIM, that is, the (q_1, p_1) surface, have linear saddle like dynamics. For a two degree-of-freedom system, this NHIM is more commonly referred in the literature as an unstable periodic orbit.

In order to understand the relationship between the NHIM and the index 1 saddle point, we note that for $H_r = 0$ and $H_b = 0$ the NHIM reduces to the point $(q_1, p_1, q_2, p_2) = (0,0,0,0)$, which is the index-1

saddle point on the energy surface $H_r + H_b = 0$. Therefore, as the total energy is increased from 0, with H_b increasing from zero, the NHIM "grows" from the index-1 saddle point on the zero energy surface into an invariant 1-sphere. This shows how the "influence" of the index-1 saddle point is carried to higher energy sufaces on which the saddle point does not exist.

The stable and unstable manifolds of the NHIM are given by

$$\mathcal{W}^{\mathrm{u}}(\mathcal{M}(h)) = \left\{(q_1, p_1, q_2, p_2) \mid q_1 = p_1, \frac{\omega_2}{2}\left(p_2^2 + q_2^2\right) = H_b > 0\right\}, \tag{2}$$

$$\mathcal{W}^{\mathrm{s}}(\mathcal{M}(h)) = \left\{(q_1, p_1, q_2, p_2) \mid q_1 = -p_1, \frac{\omega_2}{2}\left(p_2^2 + q_2^2\right) = H_b > 0\right\}, \tag{3}$$

which is two dimensional surface and have geometry $\mathbb{R} \times \mathbb{S}^1$ for a fixed energy. Thus, the codimension-1 geometry of the manifolds partition the phase space into "reactive" and "non-reactive" trajectories as shown in Fig.

$$fig : ps\_struct\_quad\_ham2dof$$

. The detailed visualization is only possible for the two degrees-of-freedom system which is also the starting point for testing the Lagrangian descriptor based approach for detecting the phase space structures.
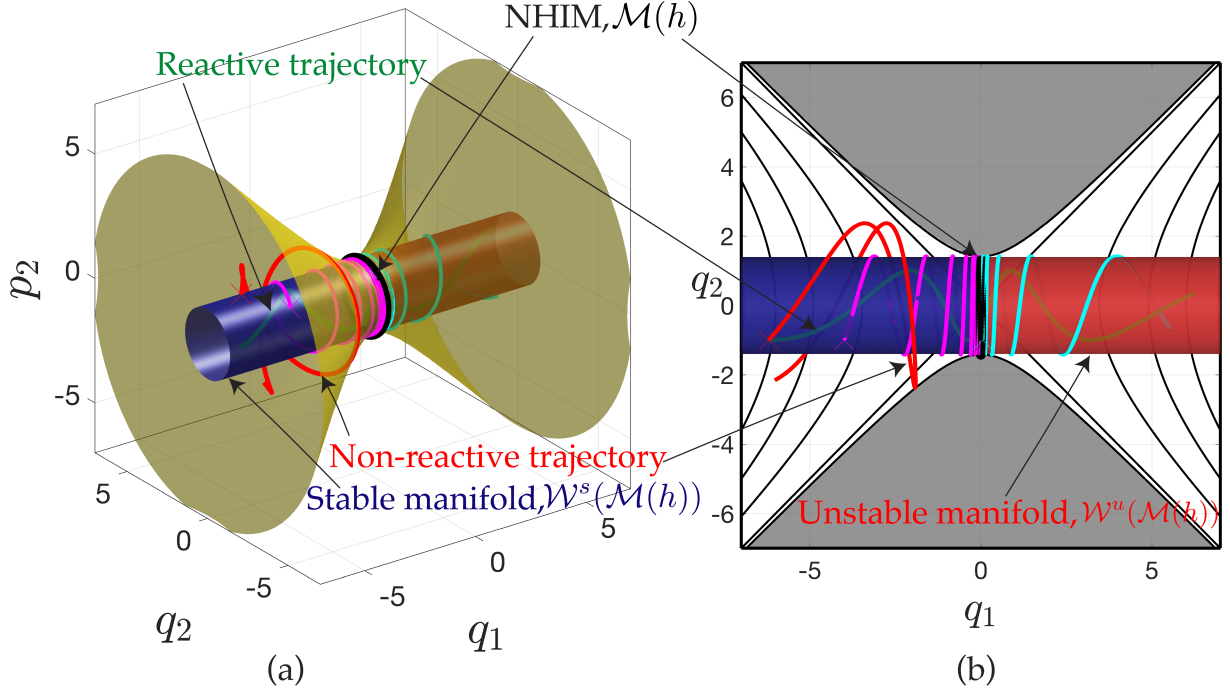

Figure 1: (a) Shows the phase space structures, namely the NHIM which is an unstable periodic orbit (as black circle), its stable and unstable manifolds (blue and red surfaces), and the energy surface (as yellow surface) for the two degrees-of-freedom decoupled quadratic Hamiltonian . Four example trajectories illustrate the dynamics mediated by these phase space structures: the red and green trajectories have the same initial configuration space coordinates, but are located outside and inside the codimension-1 invariant manifolds which separate the "reactive" (green) and "non-reactive" (red) trajectories. Also shown are the two trajectories on the manifolds (magenta on the stable manifold and cyan on the unstable manifold) that show the dynamics on the invariant surfaces. (b) Shows the projection of the stable (blue) and unstable (red) manifolds in the configuration space coordinates (q_1, q_2) along with the projection of the four example trajectories. The equipotential contours are the black lines and the region of inaccessible motion is shadded as grey.[]{data-label="fig:ps_struct_quad_ham2dof"}

Detecting the unstable periodic orbit and its manifolds

To identify NHIM and its invariant manifolds, we compute the Lagrangian descriptor in a square domain of size 2 units around the origin and discretize the coordinates of the two-dimensional surface. Next, we pick a constant value for one of the two remaining coordinates, and use the total energy equation to solve for the fourth coordinate. Due to the form of the Hamiltonian , obtaining the coordinate from the constant energy condition reduces simply to solving a quadratic equation.

- Isoenergetic two-dimensional surface parametrized by (q_1, p_1) On the constant energy surface, $H(q_1, p_1, q_2, p_2) = h$, we compute Lagrangian descriptor on a two-dimensional surface parametrized by (q_1, p_1) coordinates by defining

$$U^+_{q_1 p_1} = \{(q_1, p_1, q_2, p_2) \mid q_2 = 0, \dot{q}_2 > 0 : p_2(q_1, p_1, q_2; h) > 0\}$$

where

$$p_2(q_1, p_1, q_2 = 0; h) = \sqrt{\frac{2}{\omega_2}\left(h - \frac{\lambda}{2}(p_1^2 - q_1^2)\right)}$$

The intersection of the two-dimensional surface $U^+_{q_1 p_1}$ with the NHIM becomes

$$\mathcal{M}(h) \cap U^+_{q_1 p_1} = \{(q_1, p_1, q_2, p_2) \mid \ p_1 = 0, q_1 = 0, q_2 = 0, \dot{q}_2 > 0 :$$
$$p_2(q_1, p_1, q_2; h) > 0\}.$$

Thus, the NHIM is located at the origin $(0, 0)$ and marked by a red cross in the LD plot (Fig.

$$fig : LD\_SQH\_2dof\_q1p1$$

). Furthermore, the intersection of the two-dimensional surface with the unstable and stable manifolds is given by

$$\mathcal{W}^u(\mathcal{M}(h)) \cap U^+_{q_1 p_1} = \{(q_1, p_1, q_2, p_2) \mid \ p_1 = q_1, q_2 = 0, \dot{q}_2 > 0 :$$
$$p_2(q_1, p_1, q_2; h) > 0\},$$
$$\mathcal{W}^s(\mathcal{M}(h)) \cap U^+_{q_1 p_1} = \{(q_1, p_1, q_2, p_2) \mid \ p_1 = -q_1, q_2 = 0, \dot{q}_2 > 0 :$$
$$p_2(q_1, p_1, q_2; h) > 0\},$$

which are one-dimensional for a fixed energy, and represent lines passing through the origin shown as dashed red (unstable) and white (stable) lines, respectively, in Fig.

$$fig : LD\_SQH\_2dof\_q1p1$$

. The only points of local minima in the LD plot (Fig.

$$fig : LD\_SQH\_2dof\_q1p1$$

) also lie along the lines passing through the origin and correspond to the manifolds of the NHIM.
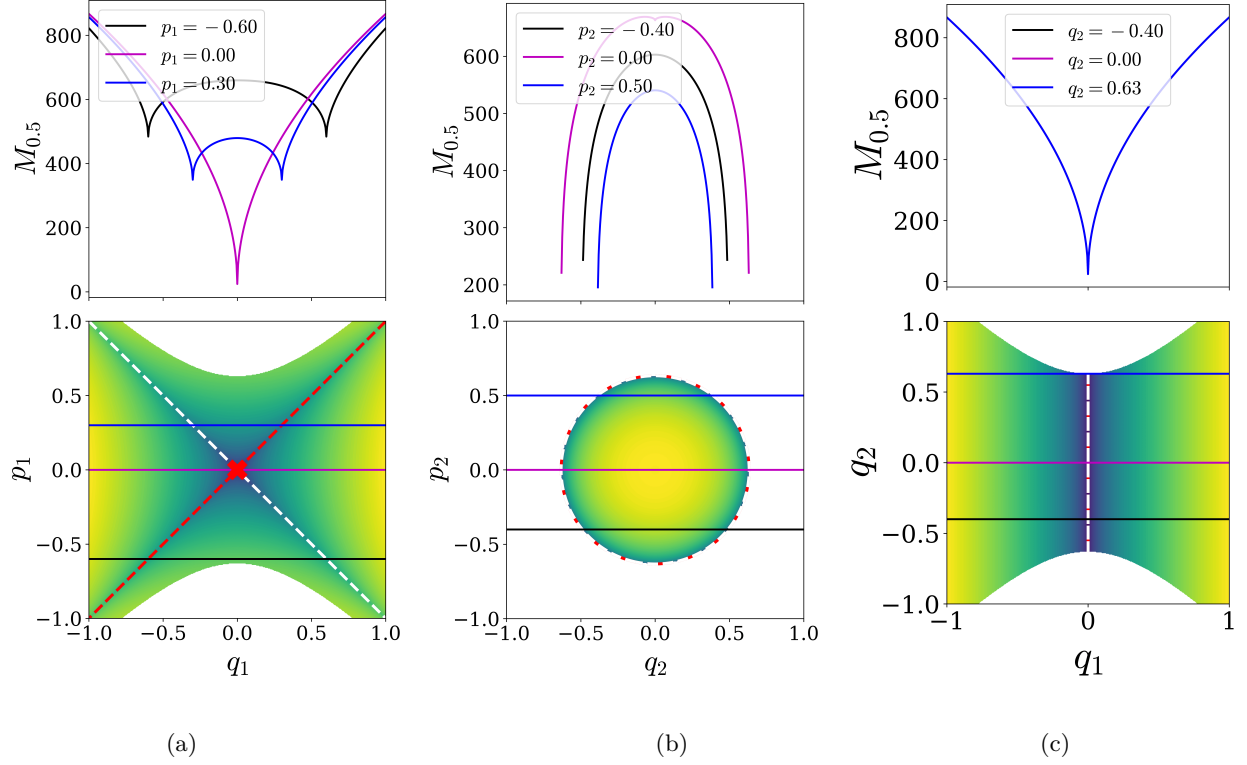
Figure 2: Lagrangian descriptor slice for the two degrees-of-freedom separable quadratic Hamiltonian on the isoenergetic two-dimensional surfaces (a) $U^+_{q_1 p_1}$, (b) $U^+_{q_2 p_2}$, (c) $U^+_{q_1 q_2}$. Parameters used are $\lambda = 1.0, \omega_2 = 1.0$ for constant total energy $H_2 = 0.2$ and integration time $\tau = 10$ is fixed.

- Isoenergetic two-dimensional surface parametrized by (q_2, p_2) Next, on the fixed energy surface, $H(q_1, p_1, q_2, p_2) = h$, we compute the Lagrangian descriptor on a two-dimensional surface parametrized by (q_2, p_2) coordinates by defining

$$U^+_{q_2 p_2} = \{(q_1, p_1, q_2, p_2) \mid q_1 = 0, \dot{q}_1 \geqslant 0 : p_1(q_1, q_2, p_2; h) \geqslant 0\}$$

where

$$p_1(q_1 = 0, q_2, p_2; h) = \sqrt{\frac{2}{\lambda}\left(h - \frac{\omega_2}{2}\left(p_2^2 + q_2^2\right)\right)}$$

The intersection of the two-dimensional surface $U^+_{q_2 p_2}$ with the NHIM is given by

$$\mathcal{M}(h) \cap U^+_{q_2 p_2} = \{(q_1, p_1, q_2, p_2) \mid p_1 = 0, q_1 = 0, \dot{q}_1 > 0,$$
$$\frac{\omega_2}{2}\left(p_2^2 + q_2^2\right) = h\}.$$

which represents a circle of radius $\sqrt{2h/\omega_2}$. The radius is ≈ 0.632 for $h = 0.2, \omega_2 = 1.0$ and is marked as a dashdot red circle in Fig.

$$fig : LD\_SQH\_2dof\_q2p2$$

. The points on the circle are also locations of minima as shown by the one-dimensional slices at constant p_2.

Next, intersection of the two-dimensional $U^+_{q_2 p_2}$ with the stable and unstable manifolds is given by

7

$$\mathcal{W}^u(\mathcal{M}(h)) \cap U^+_{q_2 p_2} = \{(q_1, p_1, q_2, p_2) \mid p_1 = q_1, q_1 = 0, \dot{q}_1 > 0 :$$
$$\frac{\omega_2}{2}\left(p_2^2 + q_2^2\right) = h\},$$

$$\mathcal{W}^s(\mathcal{M}(h)) \cap U^+_{q_2 p_2} = \{(q_1, p_1, q_2, p_2) \mid p_1 = -q_1, q_1 = 0, \dot{q}_1 > 0 :$$
$$\frac{\omega_2}{2}\left(p_2^2 + q_2^2\right) = h\},$$

which are circles of same radius $\sqrt{2h/\omega_2}$. These manifolds are identified along the boundary of the LD plot in Fig.

$$fig : LD\_SQH\_2dof\_q2p2$$

along which the minima also occurs.

- Isoenergetic two-dimensinal surface parametrized by (q_1, q_2) Next, on the constant energy surface, $H(q_1, p_1, q_2, p_2) = h$, we compute the Lagrangian descriptor on a two-dimensional surface by defining

$$U^+_{q_1 q_2} = \{(q_1, p_1, q_2, p_2) \mid p_1 = 0, p_2(q_1, p_1, q_2; h) > 0\}$$

where

$$p_2(q_1, p_1 = 0, q_2; h) = \sqrt{\frac{2}{\omega_2}\left(h + \frac{\lambda}{2}q_1^2 - \frac{\omega_2}{2}q_2^2\right)}$$

The intersection of the NHIM with the two-dimensional surface $U^+_{q_1 q_2}$ is

$$\mathcal{M}(h) \cap U^+_{q_1 q_2} = \{(q_1, p_1, q_2, p_2) \mid p_1 = 0, q_1 = 0, p_2 > 0 :$$
$$\frac{\omega_2}{2}\left(p_2^2 + q_2^2\right) = h\}.$$

which represent points on the line $q_1 = 0$ which is marked by the dashdot line in Fig.

$$fig : LD\_SQH\_2dof\_q1q2$$

.

Next, intersection of the two-dimensional $U^+_{q_1 q_2}$ with the stable and unstable manifolds is given by

$$\mathcal{W}^u(\mathcal{M}(h)) \cap U^+_{q_1 q_2} = \{(q_1, p_1, q_2, p_2) \mid p_1 = q_1, p_1 = 0, p_2 > 0 :$$
$$\frac{\omega_2}{2}\left(p_2^2 + q_2^2\right) = h\}, \tag{4}$$

$$\mathcal{W}^s(\mathcal{M}(h)) \cap U^+_{q_1 q_2} = \{(q_1, p_1, q_2, p_2) \mid p_1 = -q_1, p_1 = 0, p_2 > 0 :$$
$$\frac{\omega_2}{2}\left(p_2^2 + q_2^2\right) = h\}, \tag{5}$$

which denote lines parallel to the q_2 axis and marked by the dashed red (unstable) and white (stable) lines in Fig.

$$fig : LD\_SQH\_2dof\_q1q2$$

. These manifolds are identified by minima in the Lagrangian descriptor plot in Fig.

$$fig : LD\_SQH\_2dof\_q1q2$$

as also shown in the one-dimensional slice for constant q_2.

Now the question is how do these phase space structures manifest when the system is non-separable into "reactant" and "product" coordinates. We will answer this using a linear symplectic transformation of the separable quadratic Hamiltonian and then compute the LD on different 2D surfaces for a fixed energy.

Coupled quadratic Hamiltonian

To couple the coordinates in the separable quadratic Hamiltonian , we introduce a linear transformation, C, such that it satisfies the symplectic condition

$$C \mathcal{J} C^T = \mathcal{J} = \begin{pmatrix} 0_N & I_N \\ -I_N & 0_N \end{pmatrix}$$

where $\mathcal{J}$ is the 2N × 2N matrix and I_N denotes the $N \times N$ identity matrix. The symplectic transformation C acts on the non-separable (coupled) coordinates (x, y, p_x, p_y) to give the decoupled coordinates (q_1, q_2, p_1, p_2):

$$\begin{bmatrix} q_1 \\ q_2 \\ p_1 \\ p_2 \end{bmatrix} = C \begin{bmatrix} x \\ y \\ p_x \\ p_y \end{bmatrix} \implies \begin{bmatrix} \dot{q}_1 \\ \dot{q}_2 \\ \dot{p}_1 \\ \dot{p}_2 \end{bmatrix} = C \begin{bmatrix} \dot{x} \\ \dot{y} \\ \dot{p}_x \\ \dot{p}_y \end{bmatrix}, \quad \begin{bmatrix} \dot{x} \\ \dot{y} \\ \dot{p}_x \\ \dot{p}_y \end{bmatrix} = -C \begin{bmatrix} \dot{q}_1 \\ \dot{q}_2 \\ \dot{p}_1 \\ \dot{p}_2 \end{bmatrix}$$

since, C satisfies $C^T = C^{-1} = -C$ and some examples are given in Appendix

$$sect : examples\_C$$

.

Let us consider the symplectic transformation

$$C = \begin{pmatrix} 0 & 0 & 1 & 0 \\ 0 & 0 & 0 & 1 \\ -1 & 0 & 1 & 1 \\ 0 & -1 & 1 & 1 \end{pmatrix}$$

The coupled (non-separable) coordinates become

$$q_1 = p_x$$
$$q_2 = p_y$$
$$p_1 = -x + p_x + p_y$$
$$p_2 = -y + p_x + p_y$$

This set of transformed coordinates applied to gives the non-separable quadratic Hamiltonian

$$\mathcal{H}(x, p_x, y, p_y) = \frac{\lambda}{2} x^2 + \frac{\omega_2}{2} y^2 + \frac{\omega_2}{2} \left(2p_y^2 + p_x^2 + 2p_x p_y - 2y p_x - 2y p_y \right) + \frac{\lambda}{2} \left(p_y^2 + 2p_x p_y - 2x p_x - 2x p_y \right)$$

which gives the Hamiltonian vector field

$$\dot{x} = -\lambda x - \omega_2 y + \omega_2 p_x + (\lambda + \omega_2) p_y$$
$$\dot{p}_x = \lambda(-x + p_x + p_y)$$
$$\dot{y} = -\lambda x - \omega_2 y + (\lambda + \omega_2) p_x + (\lambda + 2\omega_2) p_y$$
$$\dot{p}_y = \omega_2(-y + p_x + p_y)$$

where the equilibrium point is at $(0, 0, 0, 0)$, and its total energy is 0. The Jacobian at this equilibrium point has eigenvalues of type $\lambda, -\lambda, i\omega_2, -i\omega_2$ (as shown in the Appendix

$$sect : linear\_symp\_transf\_jac$$

) and is of saddle × center type, that is index-1.

9

In the decoupled (separable) quadratic Hamiltonian, the dividing surface is given by $q_1 = 0$ Eqn. which in the transformed coordinates becomes $p_x = 0$. The dividing surface on the fixed energy surface $\mathcal{H} = h$ is given by

$$\mathrm{DS} = \left\{ (x, p_x, y, p_y) \,|\, \frac{\lambda}{2}p_y^2 + \omega_2 p_y^2 - \lambda x p_y - \omega_2 y p_y + \frac{\lambda}{2}x^2 + \frac{\omega_2}{2}y^2 = h \right\}. \tag{6}$$

In the decoupled coordinates, the NHIM is defined by $q_1 = 0, p_1 = 0$ on a fixed energy surface, which gives $-x + p_x + p_y = 0$ that is $p_y = x$ in the coupled coordinates, and is given by

$$\mathcal{M}(h) = \left\{ (x, p_x, y, p_y) \,|\, p_x = 0, p_y = x, \omega_2 x^2 - \omega_2 xy + \frac{\omega_2}{2}y^2 = h \right\}. \tag{7}$$

Next, in the coupled coordinates, the stable and unstable manifolds of the NHIM are given by

$$\mathcal{W}^{\mathrm{u}}(\mathcal{M}(h)) = \left\{ (x, p_x, y, p_y) \,|\, x = p_y, \frac{\omega_2}{2}\left((-y + p_x + p_y)^2 + p_y^2\right) = h > 0 \right\} \tag{8}$$

$$\mathcal{W}^{\mathrm{s}}(\mathcal{M}(h)) = \left\{ (x, p_x, y, p_y) \,|\, x = 2p_x + p_y, \frac{\omega_2}{2}\left((-y + p_x + p_y)^2 + p_y^2\right) = h > 0 \right\} \tag{9}$$

Invertible linear symplectic transformations are clearly C^∞ diffeomorphisms. They not only preserve the Hamiltonian structure, but they preserve the phase space structures relevant to reaction dynamics. In particular, Lyapunov exponents are preserved under symplectic diffeomorphisms which implies that normal hyperbolicity is preserved. The no-recrossing property of the dividing surface is a result of transversality of the Hamiltonian vector field to the dividing surface, and such transversality properties are preserved under diffeomorphisms. Hence the NHIM also has a geometry $\mathbb{S}^1$ and the invariant manifolds and are also of geometry $\mathbb{R} \times \mathbb{S}^1$.

Detecting the unstable periodic orbit and its manifolds

Now we illustrate the procedure for detecting the unstable periodic orbit, its stable and unstable manifolds by computing the Lagrangian descriptor on isoenergetic two-dimensional surfaces parametrized by a pair of coordinates of the separable quadratic Hamiltonian .

- Isoenergetic two-dimensional surface parametrized by (x, p_x) On a fixed energy surface, $\mathcal{H}(x, p_x, y, p_y) = h$, we consider a two-dimensional surface parametrized by (x, p_x) coordinates by defining

$$U_{xp_x}^+ = \left\{ (x, p_x, y, p_y) \,|\, y = 0, \ p_y = p_y(x, p_x, y; h) : \dot{y}(x, p_x, y, p_y) > 0 \right\},$$

Combining the dividing surface condition $p_x = 0$, NHIM condition $p_y = x$, the directionality condition $\dot{y}(x, y, p_x, p_y; h) > 0$, gives $x > 0$. Thus, for a fixed energy, the intersection of the one-dimensional NHIM with the isoenergetic two-dimensional surface is given by

$$\mathcal{M}(h) \cap U_{xp_x}^+ = \left\{ (x, p_x, y, p_y) \,|\, y = 0, p_x = 0, p_y = x, \right.$$
$$\left. \omega_2 x^2 - \omega_2 xy + \frac{\omega_2}{2}y^2 = h : x > 0 \right\}$$

which is a point on the line $p_x = 0$ and $x = \sqrt{2h/\omega_2}$, and is marked by the red cross in Fig.

$$fig : LD\_NSQH\_2dof\_xpx$$

. This point is also identified by the minimum value of the Lagrangian descriptor at this coordinate (as shown along the one-dimensional slice at constant $p_x = 0$) and agrees with to within the grid resolution used for

the discretization of the two-dimensional surface. Since the NHIM is the intersection of stable and unstable manifolds, its coordinate is also a minimum and singular point in the LD values.

Next, the intersection of the unstable and stable manifolds with the isoenergetic two-dimensional surface $U_{xp_x}^+$ is given by

$$\mathcal{W}^{\mathrm{u}}(\mathcal{M}(h)) \cap U_{xp_x}^+ = \{(x, p_x, y, p_y) \mid y = 0, x = p_y,$$
$$\frac{\omega_2}{2}\left((x + p_x)^2 + x^2\right) = h : (\lambda + \omega_2)p_x + 2\omega_2 x > 0\}$$
$$\mathcal{W}^{\mathrm{s}}(\mathcal{M}(h)) \cap U_{xp_x}^+ = \{(x, p_x, y, p_y) \mid y = 0, x = 2p_x + p_y,$$
$$\frac{\omega_2}{2}\left((x - p_x)^2 + (x - 2p_x)^2\right) = h : (\lambda + 3\omega_2)p_x - 2\omega_2 x < 0\}$$

where the inequalities are derived from the directionality condition $\dot{y} > 0$ for the surface. This is detected by the minima in the LD plot in Fig.

$$fig : LD\_NSQH\_2dof\_xpx$$

and highlighted by the dashed red (unstable) and dashed white (stable) curves. Points on these manifolds are also picked up by the one-dimensional slices along the constant $p_x = -0.60, 0.30$.

- Isoenergetic two-dimensional surface parametrized by (x, y) On a fixed energy surface $\mathcal{H}(x, p_x, y, p_y) = h$, we compute the Lagrangian descriptor on a two-dimensional surface parametrized by (x, y) coordinates by defining

$$U_{xy}^+ = \{(x, p_x, y, p_y) \mid p_x = 0, \ p_y(x, p_x, y; h) > 0 : \dot{p}_x(x, y, p_y) \geqslant 0\},$$

Thus, the intersection of the NHIM with this isoenergetic two-dimensional surface is given by

$$\mathcal{M}(h) \cap U_{xy}^+ = \{(x, p_x, y, p_y) \mid p_y = x, p_x = 0, p_y > 0 : p_y \geqslant x,$$
$$\omega_2 x^2 - \omega_2 xy + \frac{\omega_2}{2}y^2 = h\}$$

which represents a one-dimensional curve and is marked as a dashdot red line in Fig.

$$fig : LD\_NSQH\_2dof\_xy$$

. The NHIM is also identified by the minima in Lagrangian descriptor values along one-dimensional sections at constant y in Fig.

$$fig : LD\_NSQH\_2dof\_xy$$

.

Next, the intersection of the unstable and stable manifolds with the isoenergetic two-dimensional surface U_{xy}^+ is given by

$$\mathcal{W}^{\mathrm{u}}(\mathcal{M}(h)) \cap U_{xy}^+ = \{(x, p_x, y, p_y) \mid x = p_y, p_x = 0, p_y > 0 : p_y \geqslant x,$$
$$\omega_2 x^2 - \omega_2 xy + \frac{\omega_2}{2}y^2 = h\}$$
$$\mathcal{W}^{\mathrm{s}}(\mathcal{M}(h)) \cap U_{xy}^+ = \{(x, p_x, y, p_y) \mid x = 2p_x + p_y, p_x = 0, p_y > 0 : p_y \geqslant x,$$
$$\omega_2 x^2 - \omega_2 xy + \frac{\omega_2}{2}y^2 = h\}$$

where each manifold represents the same one-dimensional curve as the NHIM and are marked by dashed red (unstable) and dashed white (stable) lines in the Fig.

$$fig : LD\_NSQH\_2dof\_xy$$

11

. These manifolds are also identified by points of minima in the Lagrangian descriptor values as shown by one-dimensional sections at constant y values.

- Isoenergetic two-dimensional surface parametrized by (y, p_y) On the fixed energy surface $\mathcal{H}(x, p_x, y, p_y) = h$, we take the Lagrangian descriptor slice by defining a two-dimensional surface

$$U_{yp_y}^+ = \{(x, p_x, y, p_y) \mid x = 0, \ p_x(x, y, p_y; h) > 0 : \dot{x}(x, p_x, y, p_y) > 0\}$$

Thus, the intersection of the NHIM with this isoenergetic two-dimensional surface is given by

$$\mathcal{M}(h) \cap U_{yp_y}^+ = \{(x, p_x, y, p_y) \mid \ x = 0, p_y = x, p_x = 0, \dot{x}(x, p_x, y, p_y) > 0 : y < 0$$
$$\frac{\omega_2}{2} y^2 = h\}$$

which is a point $y = \sqrt{2h/\omega_2}$ on the $p_y = 0$ line and shown as a red cross in Fig.

$$fig : LD\_NSQH\_2dof\_ypy$$

. This point is also identified by the minima in the Lagrangian descriptor values as shown along one-dimensional slice in Fig.

$$fig : LD\_NSQH\_2dof\_ypy$$

.

Next, the intersection of the unstable and stable manifolds with the isoenergetic surface $U_{yp_y}^+$ manifest as

$$\mathcal{W}^{\mathrm{u}}(\mathcal{M}(h)) \cap U_{yp_y}^+ = \{(x, p_x, y, p_y) \mid \ x = 0, x = p_y, \dot{x}(x, p_x, y, p_y) > 0 : y - p_x < 0,$$
$$\frac{\omega_2}{2} (-y + p_x)^2 = h\}$$
$$\mathcal{W}^{\mathrm{s}}(\mathcal{M}(h)) \cap U_{yp_y}^+ = \{(x, p_x, y, p_y) \mid \ x = 0, x = 2p_x + p_y,$$
$$\dot{x}(x, p_x, y, p_y) > 0 : -\omega_2 y + (\frac{\omega_2}{2} + \lambda) p_y > 0,$$
$$\frac{\omega_2}{2} \left((-y + \frac{p_y}{2})^2 + p_y^2\right) = h\}$$

which are shown as dashed red (unstable) and dashed white (stable) curves in the Fig.

$$fig : LD\_NSQH\_2dof\_ypy$$

. These curves are also identified by the points of minima in the Lagrangian descriptor values as evident by the one-dimensional slices in Fig.

$$fig : LD\_NSQH\_2dof\_ypy$$

.

Three Degrees of Freedom

In this section we use the Lagrangian Descriptor method to identify the NHIM and its stable and unstable manifolds for a 3 DoF separable quadratic Hamiltonian with an index-1 saddle point at the origin. The advantage of using this model Hamiltonian is that we can compare the analytical expressions for the phase space structures present with features in LD plots.

Decoupled quadratic Hamiltonian

We consider the three degrees of freedom benchmark example in Ref.(Wiggins 2016) which is a linear system (quadratic Hamiltonian) with an equilibrium point of saddle-center-center equilibrium type at the origin. The Hamiltonian of this system is of the form

$$H = \underbrace{\frac{\lambda}{2}\left(p_1^2 - q_1^2\right)}_{H_r} + \underbrace{\frac{\omega_2}{2}\left(p_2^2 + q_2^2\right)}_{H_{b_1}} + \underbrace{\frac{\omega_3}{2}\left(p_3^2 + q_3^2\right)}_{H_{b_2}}, \quad \lambda,\, \omega_2,\, \omega_3 > 0 \tag{10}$$

with the corresponding Hamiltonian vector field given by:

$$\dot{q}_1 = \frac{\partial H}{\partial p_1} = \lambda p_1, \tag{11}$$

$$\dot{p}_1 = -\frac{\partial H}{\partial q_1} = \lambda q_1, \tag{12}$$

$$\dot{q}_2 = \frac{\partial H}{\partial p_2} = \omega_2 p_2, \tag{13}$$

$$\dot{p}_2 = -\frac{\partial H}{\partial q_2} = -\omega_2 q_2, \tag{14}$$

$$\dot{q}_3 = \frac{\partial H}{\partial p_3} = \omega_3 p_3, \tag{15}$$

$$\dot{p}_3 = -\frac{\partial H}{\partial q_3} = -\omega_3 q_3, \tag{16}$$

Since the total Hamiltonian decouples into the independent Hamiltonians H_r, H_{b_1} and H_{b_2} we can analyze the phase portraits for each separately. In the language of chemical reaction dynamics H_r corresponds to the "reactive mode", H_{b_1} and H_{b_2} are "bath modes". The equilibrium point $(q_1, p_1, q_2, p_2, q_3, p_3) = (0, 0, 0, 0, 0, 0)$ is an index-1 saddle point for the full three DoF system on the zero (total) energy surface.

In this system a trajectory "reacts" when its q_1 coordinate changes sign. Therefore the surface $q_1 = 0$ is a [*dividing surface*]{} (DS) for trajectories, separating "reactants" from "products" (i.e. before and after reaction). This DS is a five dimensional surface in the six dimensional phase space. We discuss its geometrical structure, in both the phase space and in a fixed energy surface, in more detail.

First, we consider the "energetics" of the reaction. In order for q_1 to change sign we must have $H_r > 0$. Also, it is clear from the form of H_{b_1} and H_{b_2} that $H_{b_1} \geqslant 0$ and $H_{b_2} \geqslant 0$. Therefore, reaction requires $H = H_r + H_{b_1} + H_{b_2} > 0$.

The energy surface in which reaction occurs is given by

$$\frac{\lambda}{2}\left(p_1^2 - q_1^2\right) + \frac{\omega_2}{2}\left(p_2^2 + q_2^2,\right) + \frac{\omega_3}{2}\left(p_3^2 + q_3^2,\right) = H_r + H_{b_1} + H_{b_2} = H > 0, \quad H_r > 0,\, H_{b_1},\, H_{b_2} \geqslant 0.$$

The intersection of the DS, $q_1 = 0$, with this energy surface is given by:

$$\frac{\lambda}{2}p_1^2 + \frac{\omega_2}{2}\left(p_2^2 + q_2^2,\right) + \frac{\omega_3}{2}\left(p_3^2 + q_3^2,\right) = H_r + H_{b_1} + H_{b_2} = H > 0, \quad H_r > 0,\, H_{b_1},\, H_{b_2} \geqslant 0.$$

This is the isoenergetic DS. It is a 4-sphere in the six dimensional $(q_1, p_1, q_2, p_2, q_3, p_3)$ phase space. It has two hemispheres that are DSs for the forward and backward reactions, respectively:

$$\frac{\lambda}{2}p_1^2 + \frac{\omega_2}{2}\left(p_2^2 + q_2^2,\right) + \frac{\omega_3}{2}\left(p_3^2 + q_3^2,\right) = H_r + H_{b_1} + H_{b_2} = H > 0, \quad p_1 > 0, \quad \text{forward DS},$$

$$\frac{\lambda}{2}\,p_1^2 + \frac{\omega_2}{2}\left(p_2^2 + q_2^2,\right) + \frac{\omega_3}{2}\left(p_3^2 + q_3^2,\right) = H_r + H_{b_1} + H_{b_2} = H > 0, \quad p_1 < 0, \quad \text{backward DS.}$$

Thes two hemispheres "meet" at $p_1 = 0$:

$$\frac{\omega_2}{2}\left(p_2^2 + q_2^2,\right) + \frac{\omega_3}{2}\left(p_3^2 + q_3^2,\right) = H_{b_1} + H_{b_2} \geqslant 0, \quad \text{NHIM,}$$

which is a [*normally hyperbolic invariant 3 sphere*]{}. [*invariance*]{} follows from since for $q_1 = p_1 = 0$ then $\dot{q}_1 = \dot{p}_1 = 0$. Thus q_1 and p_1 always remain zero, and trajectories with these initial conditions remain on , i.e., $q_1 = p_1 = 0$ is invariant. It is [*normally hyperbolic*]{} since the directions normal to , i.e. $q_1 - p_1$, are linearized saddle like dynamics.

In order to understand the relationship between the NHIM and the index-1 saddle point we note that for $H_r = 0$, $H_{b_1} = 0$ and $H_{b_2} = 0$ the NHIM reduces to the point $(q_1, p_1, q_2, p_2, q_3, p_3) = (0, 0, 0, 0, 0, 0)$, which is the index-1 saddle point on the energy surface $H_r + H_{b_1} + H_{b_2} = 0$. Therefore as the total energy is increased from 0, with H_{b_1} increasing from zero and/or H_{b_2} increasing from zero, we see that the NHIM "grows" from the index-1 saddle point on the zero energy surface into an invariant 3 sphere. This shows how the "influence" of the index-1 saddle point is carried to higher energy sufaces on which the saddle point does not exist.

The stable and unstable manifolds of the NHIM are given the following equations:

$$\mathcal{W}^u\left(\mathcal{M}(h)\right) = \left\{(q_1, p_1, q_2, p_2, q_3, p_3)\,|\,q_1 = p_1,\ \frac{\omega_2}{2}\left(p_2^2 + q_2^2\right) + \frac{\omega_3}{2}\left(p_3^2 + q_3^2\right) = H_{b_1} + H_{b_2} > 0\right\}, \quad (17)$$

$$\mathcal{W}^s\left(\mathcal{M}(h)\right) = \left\{(q_1, p_1, q_2, p_2, q_3, p_3)\,|\,q_1 = -p_1,\ \frac{\omega_2}{2}\left(p_2^2 + q_2^2\right) + \frac{\omega_3}{2}\left(p_3^2 + q_3^2\right) = H_{b_1} + H_{b_2} > 0\right\}, \quad (18)$$

and they are four dimensional on a fixed five dimensional energy surface. The topology of the manifolds is the product of a line ($q_1 = p_1$ or $q_1 = -p_1$) with a 3 sphere ($\frac{\omega_2}{2}\left(p_2^2 + q_2^2\right) + \frac{\omega_3}{2}\left(p_3^2 + q_3^2\right) = H_{b_1} + H_{b_2} > 0$), that is $\mathbb{R} \times \mathbb{S}^3$ and sometimes such geometry is referred to as "spherical cylinders". Since the lines $q_1 = p_1$ and $q_1 = -p_1$ correspond to the contour $H_r = 0$, in the six dimensional phase space, these manifolds have energy $H = H_r + H_{b_1} + H_{b_2} = 0 + H_{b_1} + H_{b_2} > 0$.

To understand the dynamics governed by the invariant manifolds of the NHIM, let us choose an initial condition $(q_1, p_1, q_2, p_2, q_3, p_3)$ on $\mathcal{W}^u\left(\mathcal{M}(h)\right)$. Then as $t \to +\infty$ the (q_2, p_2, q_3, p_3) components of the trajectory with this initial condition evolve quasiperiodically and the (q_1, p_1) components grow at an exponential rate. Similarly, if we choose an initial condition on $\mathcal{W}^s\left(\mathcal{M}(h)\right)$, then as $t \to +\infty$ the (q_2, p_2, q_3, p_3) components of the trajectory evolve quasiperiodically and the (q_1, p_1) components decay to zero at an exponential rate as $t \to \infty$. In other words, trajectories starting on $\mathcal{W}^u\left(\mathcal{M}(h)\right)$ decay at an exponential rate to the NHIM as $t \to -\infty$ and trajectories starting on $\mathcal{W}^s\left(\mathcal{M}(h)\right)$ decay at an exponential rate to the NHIM as $t \to +\infty$.

Detecting NHIM and its manifolds

We consider isoenergetic two-dimensional surfaces parametrized by two coordinates and compute the Lagrangian descriptor in a square domain of size 2 units around the origin. We discretize the coordinates of the two dimensional surface and pick constant values for three of the four remaining coordinates, and use the total energy equation to solve for the sixth coordinate. Due to the form of the Hamiltonian , obtaining the coordinate from the constant energy condition is simply solving a quadratic equation.

- Isoenergetic two-dimensional surface parametrized by (q_1, p_1) On the constant energy surface, $H(q_1, p_1, q_2, p_2, q_3, p_3) = h$, we compute Lagrangian descriptor on a two-dimensional surface parametrized by (q_1, p_1) coordinates by defining

$$U_{q_1 p_1}^+ = \{(q_1, p_1, q_2, p_2, q_3, p_3)\,|\ \ q_2 = 0, p_2 = 0, q_3 = 0, \dot{q}_3 > 0 :$$
$$p_3(q_1, p_1, q_2, p_2, q_3; h) > 0\}$$

where

$$p_3(q_1, p_1, q_2 = 0, p_2 = 0, q_3 = 0; h) = \sqrt{\frac{2}{\omega_3}\left(h - \frac{\lambda}{2}(p_1^2 - q_1^2)\right)}$$

The intersection of the two-dimensional surface $U_{q_1p_1}^+$ with the NHIM becomes

$$\mathcal{M}(h) \cap U_{q_1p_1}^+ = \{(q_1, p_1, q_2, p_2, q_3, p_3) \mid q_1 = 0, p_1 = 0, q_2 = 0, p_2 = 0, q_3 = 0, \dot{q}_3 > 0 : \\ p_3(q_1, p_1, q_2, p_2, q_3; h) > 0\}.$$

Thus, the NHIM is located at the origin $(0, 0)$ and marked by a red cross in the LD plot (Fig.

$$fig : LD\_SQH\_3dof\_q1p1$$

).

Next, the intersection of the two-dimensional surface with the unstable and stable manifolds is given by

$$\mathcal{W}^u(\mathcal{M}(h)) \cap U_{q_1p_1}^+ = \{(q_1, p_1, q_2, p_2, q_3, p_3) \mid q_1 = p_1, q_2 = 0, p_2 = 0, q_3 = 0, \dot{q}_3 > 0 : \\ p_3(q_1, p_1, q_2, p_2, q_3; h) > 0\},$$
$$\mathcal{W}^s(\mathcal{M}(h)) \cap U_{q_1p_1}^+ = \{(q_1, p_1, q_2, p_2, q_3, p_3) \mid q_1 = -p_1, q_2 = 0, p_2 = 0, q_3 = 0, \dot{q}_3 > 0 : \\ p_3(q_1, p_1, q_2, p_2, q_3; h) > 0\},$$

which are one-dimensional for a fixed energy, and represent lines passing through the origin shown as dashed red (unstable) and white (stable) lines, respectively, in Fig.

$$fig : LD\_SQH\_3dof\_q1p1$$

. The only points of local minima in the LD plot (Fig.

$$fig : LD\_SQH\_3dof\_q1p1$$

) also lie along the lines passing through the origin and correspond to the manifolds of the NHIM.

- Isoenergetic two-dimensional surface parametrized by (q_2, p_2) On the constant energy surface, $H(q_1, p_1, q_2, p_2, q_3, p_3) = h$, we compute Lagrangian descriptor on a two-dimensional surface parametrized by (q_2, p_2) coordinates by defining

$$U_{q_2p_2}^+ = \{(q_1, p_1, q_2, p_2, q_3, p_3) \mid q_1 = 0, q_3 = 0, p_3 = 0, \dot{q}_1 > 0 : \\ p_1(q_1, q_2, p_2, q_3, p_3; h) > 0\}$$

where

$$p_1(q_1 = 0, q_2, p_2, q_3 = 0, p_3 = 0; h) = \sqrt{\frac{2}{\lambda}\left(h - \frac{\omega_2}{2}(p_2^2 + q_2^2)\right)}$$

The intersection of the two-dimensional surface $U_{q_2p_2}^+$ with the NHIM becomes

$$\mathcal{M}(h) \cap U_{q_2p_2}^+ = \{(q_1, p_1, q_2, p_2, q_3, p_3) \mid q_1 = 0, p_1 = 0, p_3 = 0, q_3 = 0, \dot{q}_3 > 0 : \\ \frac{\omega_2}{2}(p_2^2 + q_2^2) = h\}.$$

Thus, the NHIM is the circle of radius $\sqrt{2h/\omega_2}$ and marked by a dashed line in the LD plot (Fig.

$$fig : LD\_SQH\_3dof\_q2p2$$

).

Next, the intersection of the two-dimensional surface with the unstable and stable manifolds is given by

$$\mathcal{W}^u(\mathcal{M}(h)) \cap U^+_{q_2 p_2} = \{(q_1, p_1, q_2, p_2, q_3, p_3) \mid q_1 = p_1, q_1 = 0, q_3 = 0, p_3 = 0, \dot{q}_3 > 0 :$$
$$\frac{\omega_2}{2}\left(p_2^2 + q_2^2\right) = h\},$$

$$\mathcal{W}^s(\mathcal{M}(h)) \cap U^+_{q_2 p_2} = \{(q_1, p_1, q_2, p_2, q_3, p_3) \mid q_1 = -p_1, q_1 = 0, q_3 = 0, p_3 = 0, \dot{q}_3 > 0 :$$
$$\frac{\omega_2}{2}\left(p_2^2 + q_2^2\right) = h\},$$

which are one-dimensional for a fixed energy, and marked by dashed red (unstable) and white (stable) lines, respectively, in Fig.

$$fig : LD\_SQH\_3dof\_q2p2$$

. The only points of local minima in the LD plot (Fig.

$$fig : LD\_SQH\_3dof\_q2p2$$

) also lie along the lines passing through the origin and correspond to the manifolds of the NHIM.

- Isoenergetic two-dimensional surface parametrized by (q_3, p_3) On the constant energy surface, $H(q_1, p_1, q_2, p_2, q_3, p_3) = h$, we compute Lagrangian descriptor on a two-dimensional surface parametrized by (q_3, p_3) coordinates by defining

$$U^+_{q_3 p_3} = \{(q_1, p_1, q_2, p_2, q_3, p_3) \mid p_1 = 0, q_2 = 0, p_2 = 0, \dot{p}_1 > 0 :$$
$$q_1(p_1, q_2, p_2, q_3, p_3; h) > 0\}$$

where

$$q_1(p_1 = 0, q_2 = 0, p_2 = 0, q_3, p_3; h) = \sqrt{\frac{2}{\lambda}\left(\frac{\omega_3}{2}\left(p_3^2 + q_3^2\right) - h\right)}$$

The intersection of the two-dimensional surface $U^+_{q_3 p_3}$ with the NHIM becomes

$$\mathcal{M}(h) \cap U^+_{q_3 p_3} = \{(q_1, p_1, q_2, p_2, q_3, p_3) \mid q_1 = 0, p_1 = 0, p_2 = 0, q_2 = 0, \dot{p}_1 > 0 :$$
$$\frac{\omega_3}{2}\left(p_3^2 + q_3^2\right) = h\}.$$

Thus, the NHIM is the circle of radius $\sqrt{2h/\omega_3}$ and marked by a dashed line in the LD plot (Fig.

$$fig : LD\_SQH\_3dof\_q3p3$$

).

Next, the intersection of the two-dimensional surface with the unstable and stable manifolds is given by

$$\mathcal{W}^u(\mathcal{M}(h)) \cap U^+_{q_3 p_3} = \{(q_1, p_1, q_2, p_2, q_3, p_3) \mid q_1 = p_1, p_1 = 0, q_2 = 0, p_2 = 0, \dot{p}_1 > 0 :$$
$$\frac{\omega_3}{2}\left(p_3^2 + q_3^2\right) = h\},$$

$$\mathcal{W}^s(\mathcal{M}(h)) \cap U^+_{q_3 p_3} = \{(q_1, p_1, q_2, p_2, q_3, p_3) \mid q_1 = -p_1, p_1 = 0, q_2 = 0, p_2 = 0, \dot{p}_1 > 0 :$$
$$\frac{\omega_3}{2}\left(p_3^2 + q_3^2\right) = h\},$$

which are one-dimensional for a fixed energy and represent circles of radius $\sqrt{2h/\omega_3}$, and marked by dashed red (unstable) and white (stable) lines, respectively, in Fig.

$$fig : LD\_SQH\_3dof\_q3p3$$

. The only points of minima and singularity in the LD plot (Fig.

$$fig : LD\_SQH\_3dof\_q3p3$$

) is along the circle and thus identify the manifolds of the NHIM.

- Isoenergetic two-dimensional surface parametrized by (q_1, q_2) On the constant energy surface, $H(q_1, p_1, q_2, p_2, q_3, p_3) = h$, we compute Lagrangian descriptor on a two-dimensional surface parametrized by (q_1, q_2) coordinates by defining

$$U_{q_1 q_2}^+ = \{(q_1, p_1, q_2, p_2, q_3, p_3) \mid p_1 = 0, p_2 = 0, q_3 = 0, \dot{q}_3 > 0 :$$
$$p_3(q_1, p_1, q_2, p_2, q_3; h) > 0\}$$

where

$$p_3(q_1, p_1 = 0, q_2, p_2 = 0, q_3 = 0; h) = \sqrt{\frac{2}{\omega_3} \left(h - \left(\frac{\omega_2}{2} q_2^2 - \frac{\lambda}{2} q_1^2 \right) \right)}$$

The intersection of the two-dimensional surface $U_{q_1 q_2}^+$ with the NHIM is given by

$$\mathcal{M}(h) \cap U_{q_1 q_2}^+ = \{(q_1, p_1, q_2, p_2, q_3, p_3) \mid q_1 = 0, p_1 = 0, p_2 = 0, q_3 = 0,$$
$$\frac{\omega_2}{2} q_2^2 + \frac{\omega_3}{2} p_3^2 = h : p_3(q_1, p_1, q_2, p_2, q_3; h) > 0\} .$$

Thus, on the isoenergetic two-dimensional surface $U_{q_1 q_2}^+$, the NHIM is the line $q_1 = 0$ and marked by a dashdot line in the LD plot (Fig.

$$fig : LD\_SQH\_3dof\_q1q2$$

).

Next, the intersection of the unstable and stable manifolds with two-dimensional surface is given by

$$\mathcal{W}^u(\mathcal{M}(h)) \cap U_{q_1 q_2}^+ = \{(q_1, p_1, q_2, p_2, q_3, p_3) \mid q_1 = p_1, p_1 = 0, p_2 = 0, q_3 = 0,$$
$$\frac{\omega_2}{2} q_2^2 + \frac{\omega_3}{2} p_3^2 = h : p_3(q_1, p_1, q_2, p_2, q_3; h) > 0\} ,$$
$$\mathcal{W}^s(\mathcal{M}(h)) \cap U_{q_1 q_2}^+ = \{(q_1, p_1, q_2, p_2, q_3, p_3) \mid q_1 = -p_1, p_1 = 0, p_2 = 0, q_3 = 0,$$
$$\frac{\omega_2}{2} q_2^2 + \frac{\omega_3}{2} p_3^2 = h : p_3(q_1, p_1, q_2, p_2, q_3; h) > 0\} ,$$

which are one-dimensional for a fixed energy, and marked by dashed red (unstable) and white (stable) lines, respectively, in Fig.

$$fig : LD\_SQH\_3dof\_q1q2$$

. The only points of minima in the LD plot (Fig.

$$fig : LD\_SQH\_3dof\_q1q2$$

) also lie along this line at $q_1 = 0$ and identify the manifolds of the NHIM.

- Isoenergetic two-dimensional surface parametrized by (q_2, q_3) On the constant energy surface, $H(q_1, p_1, q_2, p_2, q_3, p_3) = h$, we compute Lagrangian descriptor on a two-dimensional surface parametrized by (q_2, q_3) coordinates by defining

$$U_{q_2 q_3}^+ = \{(q_1, p_1, q_2, p_2, q_3, p_3) \mid q_1 = 0, p_2 = 0, p_3 = 0, \dot{q}_1 \geqslant 0 :$$
$$p_1(q_1, q_2, p_2, q_3, p_3; h) \geqslant 0\}$$

where

$$p_1(q_1 = 0, q_2, p_2 = 0, q_3, p_3 = 0; h) = \sqrt{\frac{2}{\lambda} \left(h - \left(\frac{\omega_2}{2} q_2^2 + \frac{\omega_3}{2} q_3^2 \right) \right)}$$

The intersection of the two-dimensional surface $U_{q_2 q_3}^+$ with the NHIM is given by

17

$$\mathcal{M}(h) \cap U_{q_2 q_3}^+ = \{(q_1, p_1, q_2, p_2, q_3, p_3) \mid q_1 = 0, p_1 = 0, p_2 = 0, p_3 = 0,$$
$$\frac{\omega_2}{2} q_2^2 + \frac{\omega_3}{2} q_3^2 = h, p_1(q_1, q_2, p_2, q_3, p_3; h) \geqslant 0\}.$$

Thus, on the isoenergetic two-dimensional surface $U_{q_2 q_3}^+$, the NHIM is an ellipse of semi-major axis $\sqrt{2h/\omega_2}$ and semi-minor axis $\sqrt{2h/\omega_3}$ if $\omega_2 < \omega_3$, and vice-versa, otherwise. In our case, $\omega_2 = \omega_3$, the intersection of the NHIM with the isoenergetic two-dimensional surface becomes a circle and marked by a dashdot line in the LD plot (Fig.

$$fig : LD\_SQH\_3dof\_q2q3$$

).

Next, the intersection of the unstable and stable manifolds with the isoenergetic two-dimensional surface is given by

$$\mathcal{W}^u(\mathcal{M}(h)) \cap U_{q_2 q_3}^+ = \{(q_1, p_1, q_2, p_2, q_3, p_3) \mid q_1 = p_1, q_1 = 0, p_2 = 0, p_3 = 0,$$
$$\frac{\omega_2}{2} q_2^2 + \frac{\omega_3}{2} q_3^2 = h, p_1(q_1, q_2, p_2, q_3, p_3; h) \geqslant 0\},$$
$$\mathcal{W}^s(\mathcal{M}(h)) \cap U_{q_2 q_3}^+ = \{(q_1, p_1, q_2, p_2, q_3, p_3) \mid q_1 = -p_1, q_1 = 0, p_2 = 0, p_3 = 0,$$
$$\frac{\omega_2}{2} q_2^2 + \frac{\omega_3}{2} q_3^2 = h, p_1(q_1, q_2, p_2, q_3, p_3; h) \geqslant 0\},$$

which have the same geometry as the NHIM on the isoenergetic two-dimensional surface, $U_{q_2 q_3}$, and marked by dashed red (unstable) and white (stable) lines, respectively, in Fig.

$$fig : LD\_SQH\_3dof\_q2q3$$

. The only points of minima in the LD plot (Fig.

$$fig : LD\_SQH\_3dof\_q2q3$$

) also lie along this circle and identify the manifolds of the NHIM.

- Isoenergetic two-dimensional surface parametrized by (q_3, q_1) On the constant energy surface, $H(q_1, p_1, q_2, p_2, q_3, p_3) = h$, we compute Lagrangian descriptor on a two-dimensional surface parametrized by (q_3, q_1) coordinates by defining

$$U_{q_3 q_1}^+ = \{(q_1, p_1, q_2, p_2, q_3, p_3) \mid q_2 = 0, p_2 = 0, p_3 = 0, \dot{q}_1 > 0 :$$
$$p_1(q_1, q_2, p_2, q_3, p_3; h) > 0\}$$

where

$$p_1(q_1, q_2 = 0, p_2 = 0, q_3, p_3 = 0; h) = \sqrt{\frac{2}{\lambda}\left(h - \left(\frac{\omega_3}{2} q_3^2 - \frac{\lambda}{2} q_1^2\right)\right)}$$

The intersection of the two-dimensional surface $U_{q_3 q_1}^+$ with the NHIM is given by

$$\mathcal{M}(h) \cap U_{q_3 q_1}^+ = \{(q_1, p_1, q_2, p_2, q_3, p_3) \mid q_1 = 0, p_1 = 0, q_2 = 0, p_2 = 0, p_3 = 0,$$
$$p_1(q_1, q_2, p_2, q_3, p_3; h) > 0, \frac{\omega_3}{2} q_3^2 = h\}.$$

which represents two points $q_3 = \pm\sqrt{2h/\omega_3}$ on the line $q_1 = 0$, and marked by a red cross in Fig.

$$fig : LD\_SQH\_3dof\_q3q1$$

. These points are also identified by the minima in the Lagrangian descriptor values as shown by one-dimensional slices at constant q_1.

Next, the intersection of the unstable and the stable manifold with the isoenergetic two-dimensional surface is given by

$$\mathcal{W}^u(\mathcal{M}(h)) \cap U^+_{q_3 q_1} = \{(q_1, p_1, q_2, p_2, q_3, p_3) \mid q_1 = p_1, q_2 = 0, p_2 = 0, p_3 = 0,$$
$$p_1(q_1, q_2, p_2, q_3, p_3; h) > 0, \frac{\omega_3}{2} q_3^2 = h\},$$

$$\mathcal{W}^s(\mathcal{M}(h)) \cap U^+_{q_3 q_1} = \{(q_1, p_1, q_2, p_2, q_3, p_3) \mid q_1 = -p_1, q_2 = 0, p_2 = 0, p_3 = 0,$$
$$p_1(q_1, q_2, p_2, q_3, p_3; h) > 0, \frac{\omega_3}{2} q_3^2 = h\},$$

where each manifold represent lines parallel to q_1 axis. The unstable manifold lies on the $q_1 > 0$ plane and the stable manifold lies on the $q_1 < 0$ plane, and are marked by dashed red (unstable) and dashed white (stable) lines in the Fig.

$$fig : LD\_SQH\_3dof\_q3q1$$

. These manifolds are again identified by points of minima in the Lagrangian descriptor values as shown by one-dimensional slices at constant q_1.

Coupled quadratic Hamiltonian

To couple the coordinates in the separable quadratic Hamiltonian , we introduce a linear transformation such that it satisfies the symplectic condition .

Let us consider the symplectic transformation

$$C = \begin{pmatrix} 0 & 0 & 0 & 1 & 0 & 0 \\ 0 & 0 & 0 & 0 & 1 & 0 \\ 0 & 0 & 0 & 0 & 0 & 1 \\ -1 & 0 & 0 & 1 & 1 & 1 \\ 0 & -1 & 0 & 1 & 1 & 1 \\ 0 & 0 & -1 & 1 & 1 & 1 \end{pmatrix}$$

The change of coordinates is given by

$$q_1 = p_x$$
$$p_1 = -x + p_x + p_y + p_z$$
$$q_2 = p_y$$
$$p_2 = -y + p_x + p_y + p_z$$
$$q_3 = p_z$$
$$p_3 = -z + p_x + p_y + p_z$$

This transformation applied to gives the Hamiltonian in the transformed coordinates

$$\mathcal{H}(x, p_x, y, p_y, z, p_z) = \frac{\lambda}{2} \left[(-x + p_x + p_y + p_z)^2 - p_x^2 \right] + \frac{\omega_2}{2} \left[(-y + p_x + p_y + p_z)^2 + p_y^2 \right]$$
$$+ \frac{\omega_3}{2} \left[(-z + p_x + p_y + p_z)^2 + p_z^2 \right]$$

which gives the vector field

$$\dot{x} = \frac{\partial \mathcal{H}}{\partial p_x} = \frac{\lambda}{2}\left[2(-x + p_x + p_y + p_z) - 2p_x\right] + \frac{\omega_2}{2}\left[2(-y + p_x + p_y + p_z)\right] + \frac{\omega_3}{2}\left[2(-z + p_x + p_y + p_z)\right] \quad (19)$$

$$= \lambda\left(-x + p_y + p_z\right) + \omega_2\left(-y + p_x + p_y + p_z\right) + \omega_3\left(-z + p_x + p_y + p_z\right) \quad (20)$$

$$\dot{p}_x = -\frac{\partial \mathcal{H}}{\partial x} \quad (21)$$

$$= \lambda\left(-x + p_x + p_y + p_z\right) \quad (22)$$

$$\dot{y} = \frac{\partial \mathcal{H}}{\partial p_y} = \frac{\lambda}{2}\left[2(-x + p_x + p_y + p_z)\right] + \frac{\omega_2}{2}\left[2p_y + 2(-y + p_x + p_y + p_z)\right] + \frac{\omega_3}{2}\left[2(-z + p_x + p_y + p_z)\right] \quad (23)$$

$$= \lambda\left(-x + p_x + p_y + p_z\right) + \omega_2\left(-y + p_x + 2p_y + p_z\right) + \omega_3\left(-z + p_x + p_y + p_z\right) \quad (24)$$

$$\dot{p}_y = -\frac{\partial \mathcal{H}}{\partial y} \quad (25)$$

$$= \omega_2\left(-y + p_x + p_y + p_z\right) \quad (26)$$

$$\dot{z} = \frac{\partial \mathcal{H}}{\partial p_z} = \frac{\lambda}{2}\left[2(-x + p_x + p_y + p_z)\right] + \frac{\omega_2}{2}\left[2(-y + p_x + p_y + p_z)\right] + \frac{\omega_3}{2}\left[2p_z + 2(-z + p_x + p_y + p_z)\right] \quad (27)$$

$$= \lambda\left(-x + p_x + p_y + p_z\right) + \omega_2\left(-y + p_x + p_y + p_z\right) + \omega_3\left(-z + p_x + p_y + 2p_z\right) \quad (28)$$

$$\dot{p}_z = -\frac{\partial \mathcal{H}}{\partial z} \quad (29)$$

$$= \omega_3\left(-z + p_x + p_y + p_z\right) \quad (30)$$

where the equilibrium point is at $(0,0,0,0,0,0)$ and its total energy is 0. The Jacobian at this equilibrium point has eigenvalues $\lambda, -\lambda, i\omega_2, -i\omega_2, i\omega_3, -i\omega_3$ (as shown in the Appendix

$$sect: linear\_symp\_transf\_jac$$

) and is saddle $\times$ center $\times$ center, thus index-1. The energy surface is a five dimensional surface given by in the six dimensional phase space.

In the decoupled (separable) system , the dividing surface is defined by $q_1 = 0$ which becomes $p_x = 0$ in the coupled (non-separable) coordinates. The dividing surface for a fixed energy $\mathcal{H}(x, p_x, y, p_y, z, p_z) = h$ is given by

$$\mathrm{DS} = \frac{\lambda}{2}\left[(-x + p_y + p_z)^2\right] + \frac{\omega_2}{2}\left[p_y^2 + (-y + p_y + p_z)^2\right] + \frac{\omega_3}{2}\left[p_z^2 + (-z + p_y + p_z)^2\right] = h,$$

On this dividing surface, the NHIM is defined by $p_1 = 0$ in the separable coordinates, which gives $-x + p_x + p_y + p_z = 0$ that is $p_y + p_z = x$ in the non-separable coordinates, and can be expressed as

$$\mathcal{M}(h) = \frac{\omega_2}{2}\left[(x - p_z)^2 + (x - y)^2\right] + \frac{\omega_3}{2}\left[p_z^2 + (x - z)^2\right] = h.$$

Next, in the coupled coordinates, the stable and unstable manifolds of the NHIM are given by

$$\mathcal{W}^{\mathrm{u}}(\mathcal{M}(h)) = \{(x, y, z, p_x, p_y, p_z) \mid x = p_y + p_z,$$
$$\frac{\omega_2}{2}\left((-y + p_x + p_y + p_z)^2 + p_y^2\right) +$$
$$\frac{\omega_3}{2}\left((-z + p_x + p_y + p_z)^2 + p_z^2\right) = h\}, \quad (31)$$

$$\mathcal{W}^{\mathrm{s}}(\mathcal{M}(h)) = \{(x, y, z, p_x, p_y, p_z) \mid x = 2p_x + p_y + p_z,$$
$$\frac{\omega_2}{2}\left((-y + p_x + p_y + p_z)^2 + p_y^2\right) +$$
$$\frac{\omega_3}{2}\left((-z + p_x + p_y + p_z)^2 + p_z^2\right) = h\} \quad (32)$$

20

As noted earlier, invertible linear symplectic transformations preserve the normal hyperbolicity and the transversality of the Hamiltonian vector field to the dividing surface. Hence the NHIM still has a geometry $\mathbb{S}^3$ and the invariant manifolds and are also $\mathbb{R} \times \mathbb{S}^3$.

Detecting NHIM and its manifolds

Now we illustrate the procedure for detecting NHIM and its stable and unstable manifolds using features in Lagrangian descriptor on isoenergetic two-dimensional surfaces for the non-separable quadratic Hamiltonian .

- Isoenergetic two-dimensional surface parametrized by (x, p_x) On the constant energy surface, $\mathcal{H}(x, p_x, y, p_y, z, p_z) = h$, we compute the Lagrangian descriptor on a two-dimensional surface parametrized by (x, p_x) coordinates by defining

$$U^+_{xp_x} = \{(x, p_x, y, p_y, z, p_z) \mid y = 0, z = 0, p_y = 0,$$
$$p_z(x, p_x, y, p_y, z; h) > 0 : \dot{z}(x, y, z, p_x, p_y, p_z) > 0\},$$

Thus, on the five-dimensional energy surface, the intersection of the three-dimensional NHIM with the two-dimensional surface is zero-dimensional and given by

$$\mathcal{M}(h) \cap U^+_{xp_x} = \{(x, p_x, y, p_y, z, p_z) \mid y = 0, z = 0, p_y = 0, p_x = 0, p_y + p_z = x,$$
$$\frac{\omega_2}{2}\left((x - p_z)^2 + x^2\right) + \frac{\omega_3}{2}\left(p_z^2 + x^2\right) = h,$$
$$\dot{z}(x, p_x, y, p_y, z, p_z) > 0 : x > 0\}.$$

which is a point on the line $p_x = 0$, and marked by a red cross in Fig.

$$fig : NSQH\_3dof\_xpx$$

. This is also identified by the location of minima in the Lagrangian descriptor values as shown by the one-dimensional slice in Fig.

$$fig : NSQH\_3dof\_xpx$$

and agrees with $x = \sqrt{2h/(\omega_2 + 2\omega_3)}$ to within the grid resolution.

Next, the intersection of the unstable and stable manifolds with the isoenergetic two-dimensional surface becomes

$$\mathcal{W}^u(\mathcal{M}(h)) \cap U^+_{xp_x} = \{(x, p_x, y, p_y, z, p_z) \mid y = 0, z = 0, p_y = 0, x = p_y + p_z,$$
$$\frac{\omega_2}{2}(x + p_x)^2 + \frac{\omega_3}{2}\left((x + p_x)^2 + x^2\right) = h,$$
$$\dot{z}(x, p_x, y, p_y, z, p_z) > 0 :$$
$$(\omega_2 + 2\omega_3)x + (\lambda + \omega_2 + \omega_3)p_x > 0\},$$
$$\mathcal{W}^s(\mathcal{M}(h)) \cap U^+_{xp_x} = \{(x, p_x, y, p_y, z, p_z) \mid y = 0, z = 0, p_y = 0, x = 2p_x + p_y + p_z,$$
$$\frac{\omega_2}{2}(x - p_x)^2 + \frac{\omega_3}{2}\left((x - p_x)^2 + (x - 2p_x)^2\right) = h,$$
$$\dot{z}(x, p_x, y, p_y, z, p_z) > 0 :$$
$$(\omega_2 + 2\omega_3)x + (-\lambda - \omega_2 - 3\omega_3)p_x > 0\}$$

which are one-dimensional and are shown as a dashed red line (unstable) and a dashed white line (stable) in Fig.

$$fig : NSQH\_3dof\_xpx$$

. These lines are also identified by the minima in the Lagrangian descriptor values as shown by one-dimensional slice at constant p_x.

- Isoenergetic two-dimensional surface parametrized by (y, p_y) On a constant energy surface, $\mathcal{H}(x, p_x, y, p_y, z, p_z) = h$, we compute Lagrangian descriptor on a two-dimensional surface by defining

$$U_{yp_y}^+ = \{(x, p_x, y, p_y, z, p_z) \mid x = 0, \ z = 0, \ p_z = 0,$$
$$p_x(x, y, p_y, z, p_z; h) > 0 : \dot{x}(x, p_x, y, p_y, z, p_z) > 0\},$$

The intersection of the NHIM with the two-dimensional surface is given by

$$\mathcal{M}(h) \cap U_{yp_y}^+ = \{(x, p_x, y, p_y, z, p_z) \mid x = 0, z = 0, p_z = 0, p_x = 0, p_y + p_z = x,$$
$$\frac{\omega_2}{2}y^2 = h, \dot{x}(x, p_x, y, p_y, z, p_z) > 0 \ : \ y < 0\}.$$

which is a point on the isoenergetic two-dimensional surface , and shown as red cross in Fig.

$$fig : NSQH\_3dof\_ypy$$

. This point is also identified by the minima in the Lagrangian descriptor values as shown by the one-dimensional slices for constant y.

Next, the intersection of the unstable and stable manifolds with the isoenergetic two-dimensional surface becomes

$$\mathcal{W}^{\mathrm{u}}(\mathcal{M}(h)) \cap U_{ypy}^+ = \{(x, p_x, y, p_y, z, p_z) \mid x = 0, z = 0, p_z = 0, x = p_y + p_z,$$
$$\frac{\omega_2}{2}(-y + p_x)^2 + \frac{\omega_3}{2}p_x^2 = h,$$
$$\dot{x}(x, p_x, y, p_y, z, p_z) > 0 \ : \ -\omega_2 y + \lambda p_y > 0\}$$
$$\mathcal{W}^{\mathrm{s}}(\mathcal{M}(h)) \cap U_{ypy}^+ = \{(x, p_x, y, p_y, z, p_z) \mid x = 0, z = 0, p_z = 0, x = 2p_x + p_y + p_z,$$
$$\frac{\omega_2}{2}\left(\left(-y + \frac{p_y}{2}\right)^2 + p_y^2\right) + \frac{\omega_3}{2}\frac{p_y^2}{4} = h :$$
$$\dot{x}(x, p_x, y, p_y, z, p_z) > 0 \ : \ -2\omega_2 y + (2\lambda + \omega_2 + \omega_3)p_y > 0\}$$

which are lines on the two-dimensional isoenergetic surface and are also identified by the minima in the Lagrangian descriptor values as shown by the one-dimensional slices at constant y.

- Isoenergetic two-dimensional surface parametrized by (z, p_z) On a constant energy surface, $\mathcal{H}(x, p_x, y, p_y, z, p_z) = h$, we compute Lagrangian descriptor on a two-dimensional surface by defining

$$U_{zp_z}^+ = \{(x, p_x, y, p_y, z, p_z) \mid x = 0, \ y = 0, \ p_y = 0,$$
$$p_x(x, y, p_y, z, p_z; h) > 0 : \dot{x}(x, p_x, y, p_y, z, p_z) > 0\}, \tag{33}$$

The intersection of the NHIM with the two-dimensional surface is given by

$$\mathcal{M}(h) \cap U_{zp_z}^+ = \{(x, p_x, y, p_y, z, p_z) \mid x = 0, y = 0, p_y = 0, p_x = 0, p_y + p_z = x,$$
$$\frac{\omega_2}{2}p_z^2 + \frac{\omega_3}{2}\left(p_z^2 + z^2\right) = h,$$
$$\dot{x}(x, p_x, y, p_y, z, p_z) > 0 \ : \ z < 0\}.$$

which is a point and shown as red cross in Fig.

$$fig : NSQH\_3dof\_zpz$$

. This point is also identified by the minima in the Lagrangian descriptor values as shown by the one-dimensional slices for constant z.

Next, the intersection of the four-dimensional unstable and stable manifolds with the isoenergetic two-dimensional surface becomes

$$
\begin{aligned}
\mathcal{W}^{\mathrm{u}}(\mathcal{M}(h)) \cap U_{zp_z}^{+} = \{(x, p_x, y, p_y, z, p_z) \mid \ & x = 0, y = 0, p_y = 0, p_z = 0, \\
& \frac{\omega_2}{2} p_x^2 + \frac{\omega_3}{2}\left((-z + p_x)^2\right) = h : \\
& \dot{x}(x, p_x, y, p_y, z, p_z) > 0 : \omega_2 p_x + \omega_3(-z + p_x) > 0\} \\
\mathcal{W}^{\mathrm{s}}(\mathcal{M}(h)) \cap U_{zp_z}^{+} = \{(x, p_x, y, p_y, z, p_z) \mid \ & x = 0, y = 0, p_y = 0, p_z + 2p_x = 0, \\
& \frac{\omega_2}{2}\left(\frac{p_z}{2}\right)^2 + \frac{\omega_3}{2}\left(\left(-z + \frac{p_z}{2}\right)^2 + p_z^2\right) = h : \\
& \dot{x}(x, p_x, y, p_y, z, p_z) > 0 : -\omega_3 z + (\lambda + \omega_2/2 + \omega_3/2)p_z > 0\}
\end{aligned}
$$

which are one-dimensional and shown as dashed red (unstable) and dashed white (stable) lines in Fig.

$$fig : NSQH\_3dof\_zpz$$

. These invariant manifolds are also identified by minima in the Lagrangian descriptor values as shown by the one-dimensional slice at constant z.

- Isoenergetic two-dimensional surface parametrized by (x, p_z) On a constant energy surface, $\mathcal{H}(x, p_x, y, p_y, z, p_z) = h$, we compute the Lagrangian descriptor on a two-dimensional surface by defining

$$
\begin{aligned}
U_{xp_z}^{+} = \{(x, p_x, y, p_y, z, p_z) \mid \ & p_x = 0, y = 0, z = 0, \\
& p_y = p_y(x, p_x, y, p_y, z; h) : \dot{y}(x, p_x, y, p_y, z, p_z) > 0\},
\end{aligned}
$$

The intersection of the NHIM with the two-dimensional surface is given by

$$
\begin{aligned}
\mathcal{M}(h) \cap U_{xp_z}^{+} = \{(x, p_x, y, p_y, z, p_z) \mid \ & p_x = 0, y = 0, z = 0, p_y + p_z = x, \\
& \frac{\omega_2}{2}\left((x - p_z)^2 + x^2\right) + \frac{\omega_3}{2}\left(p_z^2 + x^2\right) = h, \\
& \dot{y}(x, p_x, y, p_y, z, p_z) > 0 : \omega_2(2x - p_z) + \omega_3 x > 0\}.
\end{aligned}
$$

which is also identified by the minima in the Lagrangian descriptor values as shown in the one-dimensional slices at constant p_z.

Next, the intersection of the unstable and stable manifolds with the isoenergetic two-dimensional surface becomes

$$
\begin{aligned}
\mathcal{W}^{\mathrm{u}}(\mathcal{M}(h)) \cap U_{xp_z}^{+} = \{(x, p_x, y, p_y, z, p_z) \mid \ & p_x = 0, y = 0, z = 0, x = p_y + p_z, \\
& \frac{\omega_2}{2}\left(x^2 + (x - p_z)^2\right) + \frac{\omega_3}{2}\left(x^2 + p_z^2\right) = h, \\
& \dot{y}(x, p_x, y, p_y, z, p_z) > 0 : \omega_2(2x - p_z) + \omega_3 x > 0\}, \\
\mathcal{W}^{\mathrm{s}}(\mathcal{M}(h)) \cap U_{xp_z}^{+} = \{(x, p_x, y, p_y, z, p_z) \mid \ & p_x = 0, y = 0, z = 0, x = 2p_x + p_y + p_z, \\
& \frac{\omega_2}{2}\left(x^2 + (x - p_z)^2\right) + \frac{\omega_3}{2}\left(x^2 + p_z^2\right) = h, \\
& \dot{y}(x, p_x, y, p_y, z, p_z) > 0 : \omega_2(2x - p_z) + \omega_3 x > 0\}
\end{aligned}
$$

which project as the same one-dimensional curve as the NHIM and identified by the minima in the Lagrangian descriptor values as shown by the one-dimensional slices at constant p_z in Fig.

$$fig : NSQH\_3dof\_xpz$$

.

- Isoenergetic two-dimensional surface parametrized by (y, p_z) Next, on a constant energy surface, $\mathcal{H}(x, p_x, y, p_y, z, p_z) = h$, we compute Lagrangian descriptor on a two-dimensional surface by defining

$$U^+_{yp_z} = \{(x, p_x, y, p_y, z, p_z) \mid x = 0, p_x = 0, z = 0,$$
$$p_y(x, p_x, y, z, p_z; h) > 0 : \dot{x}(x, p_x, y, p_y, z, p_z) > 0\},$$

Thus, the intersection of the NHIM with the two-dimensional surface is given by

$$\mathcal{M}(h) \cap U^+_{yp_z} = \{(x, p_x, y, p_y, z, p_z) \mid x = 0, p_x = 0, z = 0, p_y + p_z = x,$$
$$\frac{(\omega_2 + \omega_3)}{2} p_z^2 + \frac{\omega_2}{2} y^2 = h,$$
$$\dot{x}(x, p_x, y, p_y, z, p_z) > 0 : y < 0\}.$$

which represents a portion of the ellipse and shown as the dashdot red curve in Fig.

$$fig : NSQH\_3dof\_ypz$$

. As shown by the one-dimensional slices for constant p_z, Eqn. is identified by the minima in the Lagrangian descriptor values.

Next, the intersection of the unstable and stable manifolds with the isoenergetic two-dimensional surface becomes

$$\mathcal{W}^{\mathrm{u}}(\mathcal{M}(h)) \cap U^+_{ypz} = \{(x, p_x, y, p_y, z, p_z) \mid x = 0, p_x = 0, z = 0, x = p_y + p_z,$$
$$\frac{\omega_2}{2} y^2 + \frac{(\omega_2 + \omega_3)}{2} p_z^2 = h,$$
$$\dot{x}(x, p_x, y, p_y, z, p_z) > 0 : y < 0\},$$
$$\mathcal{W}^{\mathrm{s}}(\mathcal{M}(h)) \cap U^+_{ypz} = \{(x, p_x, y, p_y, z, p_z) \mid x = 0, p_x = 0, z = 0, x = 2p_x + p_y + p_z,$$
$$\frac{\omega_2}{2} y^2 + \frac{(\omega_2 + \omega_3)}{2} p_z^2 = h,$$
$$\dot{x}(x, p_x, y, p_y, z, p_z) > 0 : y < 0\}$$

which are shown as red dashed line (unstable) and white dashed line (stable) in Fig.

$$fig : NSQH\_3dof\_ypz$$

. We note here that the intersection of the manifolds with the isoenergetic two-dimensional surface overlays on the NHIM's intersection . These curves are also identified by the minima in the Lagrangian descriptor values as shown by the one-dimensional slice for constant p_z.

- Isoenergetic two-dimensional surface parametrized by (x, z) Next, on a constant energy surface, $\mathcal{H}(x, p_x, y, p_y, z, p_z) = h$, we compute the Lagrangian descriptor on a two-dimensional surface by defining

$$U^+_{xz} = \{(x, p_x, y, p_y, z, p_z) \mid y = 0, p_x = 0, p_z = 0,$$
$$p_y = p_y(x, p_x, y, z, p_z; h) : \dot{p}_z(x, p_x, y, p_y, z, p_z) > 0\},$$

24

The intersection of the NHIM with the two-dimensional surface is given by

$$\text{NHIM} \cap U_{xz}^+ = \{(x, p_x, y, p_y, z, p_z) \mid y = 0, p_x = 0, p_z = 0, p_y + p_z = x,$$
$$\omega_2 x^2 + \frac{\omega_3}{2}(x - z)^2 = h,$$
$$\dot{p_z}(x, p_x, y, p_y, z, p_z) > 0 : \omega_3(-z + x) > 0\}.$$

which represents a portion of an ellipse and is identified by the minima in the Lagrangian descriptor values as shown by the one-dimensional slices for constant z in Fig.

$$fig : NSQH\_3dof\_xz$$

.

Next, the intersection of the unstable and stable manifolds with the isoenergetic two-dimensional surface becomes

$$W^{\mathrm{u}}(\text{NHIM}) \cap U_{xz}^+ = \{(x, p_x, y, p_y, z, p_z) \mid y = 0, p_x = 0, p_z = 0, x = p_y + p_z,$$
$$\omega_2 x^2 + \frac{\omega_3}{2}(-z + x)^2 = h,$$
$$\dot{p_z}(x, p_x, y, p_y, z, p_z) > 0 : \omega_3(-z + x) > 0\},$$
$$W^{\mathrm{s}}(\text{NHIM}) \cap U_{xz}^+ = \{(x, p_x, y, p_y, z, p_z) \mid y = 0, p_x = 0, p_z = 0, x = 2p_x + p_y + p_z,$$
$$\omega_2 x^2 + \frac{\omega_3}{2}(-z + x)^2 = h,$$
$$\dot{p_z}(x, p_x, y, p_y, z, p_z) > 0 : \omega_3(-z + x) > 0\}$$

which are also be identified by the minima in the Lagrangian descriptor values as shown by the one-dimensional slice for constant z in Fig.

$$fig : NSQH\_3dof\_xz$$

.

Summary and Outlook

In this article, we assessed Lagrangian descriptor (LD) based detection of high dimensional phase space structures, that is normally hyperbolic invariant manifolds, their unstable and stable manifolds, in the two and three degrees-of-freedom quadratic Hamiltonian systems with index-1 saddle. This is done using a sytematic comparison of numerical results with analytical expressions for a comprehensive set of coordinates; see Appendix

$$sect : LD\_add\_slices$$

for more pairs of coordinates that support the results herein.. It is to be noted that in N DoF system, there are $2N(2N - 1)(N - 1)$ two-dimensional sections, so the detection strategy should include inspecting a few pairs of coordinates. Based on our investigation, a judicious choice of coordinate for the two-dimensional surface is to use one of the reaction coordinates in phase space, that is q_1 or p_1, and the other one from the remaining $2N - 1$ coordinates.

The closed-form analytical expressions of the NHIM and their manifolds are precisely identified by the minima and singular features in the Lagrangian descriptor values. This provides further numerical evidence for the use of LDs in detecting high dimensional phase space structures with a simple computation that can be implemented along with trajectory integration. So at least for the form of Hamiltonian considered here, one can rely with certainty on using Lagrangian descriptor to detect the NHIM and its stable and unstable manifolds. Furthermore, this detection approach has the potential to be combined with machine learning type methods (Feldmaier et al. 2019). Future work on this approach will include specific nonlinear systems

that are inspired by applications in celestial mechanics, ship dynamics, structural mechanics, and chemical reaction dynamics.

Acknowledgements

Balibrea-Iniesta, F., C. Lopesino, S. Wiggins, and A. M. Mancho. 2016. "Lagrangian Descriptors for Stochastic Differential Equations: A Tool for Revealing the Phase Portrait of Stochastic Dynamical Systems." *International Journal of Bifurcation and Chaos* 26 (13). World Scientific: 1630036.

Banks, David. 1992. "Interactive Manipulation and Display of Surfaces in Four Dimensions." In *Proceedings of the 1992 Symposium on Interactive 3D Graphics*, 197–207. I3D '92. New York, NY, USA: ACM. doi:10.1145/147156.147205.

Bardakcioglu, Robin, Andrej Junginger, Matthias Feldmaier, Jörg Main, and Rigoberto Hernandez. 2018. "Binary Contraction Method for the Construction of Time-Dependent Dividing Surfaces in Driven Chemical Reactions." *Physical Review E* 98 (3).

Cámara, A. de la, A. M. Mancho, K. Ide, E. Serrano, and C.R. Mechoso. 2012. "Routes of transport across the Antarctic polar vortex in the southern spring." *J. Atmos. Sci.* 69 (2): 753–67.

Craven, Galen T, and Rigoberto Hernandez. 2015. "Lagrangian Descriptors of Thermalized Transition States on Time-Varying Energy Surfaces." *Physical Review Letters* 115 (14). APS: 148301.

———. 2016. "Deconstructing Field-Induced Ketene Isomerization Through Lagrangian Descriptors." *Physical Chemistry Chemical Physics* 18 (5). Royal Society of Chemistry: 4008–18.

Craven, Galen T, Andrej Junginger, and Rigoberto Hernandez. 2017. "Lagrangian Descriptors of Driven Chemical Reaction Manifolds." *Physical Review E* 96 (2). APS: 022222.

Dellnitz, M., O. Junge, W. S. Koon, F. Lekien, M. W. Lo, J. E. Marsden, K. Padberg, R. Preis, S. D. Ross, and B. Thiere. 2005. "Transport in Dynamical Astronomy and Multibody Problems." *Int. J. Bifurc. Chaos* 15: 699–727.

Demian, A. S., and S. Wiggins. 2017. "Detection of Periodic Orbits in Hamiltonian Systems Using Lagrangian Descriptors." *International Journal of Bifurcation and Chaos* 27 (14): 1750225.

Evans, M. G., and M. Polanyi. 1935. "Some Applications of the Transition State Method to the Calculation of Reaction Velocities, Especially in Solution." *Transactions of the Faraday Society* 31: 875.

Eyring, Henry. 1938. "The Theory of Absolute Reaction Rates." *Transactions of the Faraday Society* 34: 41.

Ezra, Gregory S., and Stephen Wiggins. 2018. "Sampling Phase Space Dividing Surfaces Constructed from Normally Hyperbolic Invariant Manifolds (NHIMs)." *The Journal of Physical Chemistry A* 122 (42): 8354–62.

Ezra, Gregory S., Holger Waalkens, and Stephen Wiggins. 2009. "Microcanonical Rates, Gap Times, and Phase Space Dividing Surfaces." *The Journal of Chemical Physics* 130 (16): 164118.

Feldmaier, Matthias, Andrej Junginger, Jörg Main, Günter Wunner, and Rigoberto Hernandez. 2017. "Obtaining Time-Dependent Multi-Dimensional Dividing Surfaces Using Lagrangian Descriptors." *Chemical Physics Letters* 687. Elsevier: 194–99.

Feldmaier, Matthias, Philippe Schraft, Robin Bardakcioglu, Johannes Reiff, Melissa Lober, Martin Tschöpe, Andrej Junginger, Jörg Main, Thomas Bartsch, and Rigoberto Hernandez. 2019. "Invariant Manifolds and Rate Constants in Driven Chemical Reactions." *The Journal of Physical Chemistry B* 123 (9): 2070–86. doi:10.1021/acs.jpcb.8b10541.

Gabern, F., W. S. Koon, J. E. Marsden, and S. D. Ross. 2005. "Theory and Computation of Non-RRKM

Lifetime Distributions and Rates in Chemical Systems with Three or More Degrees of Freedom." *Physica D* 211: 391–406.

Gabern, F., W. S. Koon, J. E. Marsden, S. D. Ross, and T. Yanao. 2006. "Application of Tube Dynamics to Non-Statistical Reaction Processes." *Few-Body Systems* 38: 167–72.

García-Garrido, Víctor J., Jezabel Curbelo, Ana M. Mancho, Stephen Wiggins, and Carlos R. Mechoso. 2018. "The Application of Lagrangian Descriptors to 3D Vector Fields." *Regular and Chaotic Dynamics* 23 (5): 551–68.

García-Garrido, Víctor J., Ana M. Mancho, and Stephen Wiggins. 2015. "A dynamical systems approach to the surface search for debris associated with the disappearance of flight MH370." *Nonlin. Proc. Geophys.* 22: 701–12.

Garrett, Bruce C. 2000. "Perspective on 'The Transition State Method'." *Theoretical Chemistry Accounts: Theory, Computation, and Modeling (Theoretica Chimica Acta)* 103 (3-4): 200–204.

Gottwald, J. A., L. N. Virgin, and E. H. Dowell. 1995. "Routes to escape from an energy well." *Journal of Sound and Vibration* 187 (1): 133–44.

Hoffmann, Christoph M, and Jianhua Zhou. 1991. "Some Techniques for Visualizing Surfaces in Four-Dimensional Space." *Computer-Aided Design* 23 (1). Elsevier: 83–91.

Jaffé, C., D. Farrelly, and T. Uzer. 1999. "Transition State in Atomic Physics." *Phys. Rev. A* 60: 3833–50.

Junginger, Andrej, and Rigoberto Hernandez. 2016a. "Lagrangian Descriptors in Dissipative Systems." *Physical Chemistry Chemical Physics* 18 (44): 30282–7.

———. 2016b. "Uncovering the Geometry of Barrierless Reactions Using Lagrangian Descriptors." *The Journal of Physical Chemistry B* 120 (8): 1720–5.

Junginger, Andrej, Galen T Craven, Thomas Bartsch, F Revuelta, F Borondo, RM Benito, and Rigoberto Hernandez. 2016. "Transition State Geometry of Driven Chemical Reactions on Time-Dependent Double-Well Potentials." *Physical Chemistry Chemical Physics* 18 (44). Royal Society of Chemistry: 30270–81.

Junginger, Andrej, Lennart Duvenbeck, Matthias Feldmaier, Jörg Main, Günter Wunner, and Rigoberto Hernandez. 2017. "Chemical Dynamics Between Wells Across a Time-Dependent Barrier: Self-Similarity in the Lagrangian Descriptor and Reactive Basins." *The Journal of Chemical Physics* 147 (6). AIP Publishing: 064101.

Junginger, Andrej, Jörg Main, Günter Wunner, and Rigoberto Hernandez. 2017. "Variational Principle for the Determination of Unstable Periodic Orbits and Instanton Trajectories at Saddle Points." *Physical Review A* 95 (3).

Koçak, H" useyin, Frederic Bisshopp, Thomas Banchoff, and David Laidlaw. 1986. "Topology and Mechanics with Computer Graphics." *Advances in Applied Mathematics* 7 (3): 282–308. doi:10.1016/0196-8858(86)90037-0.

Lopesino, C., F. Balibrea-Iniesta, V. J. García-Garrido, S. Wiggins, and A. M. Mancho. 2017. "A Theoretical Framework for Lagrangian Descriptors." *International Journal of Bifurcation and Chaos* 27 (01): 1730001.

Lopesino, Carlos, Francisco Balibrea, Stephen Wiggins, and Ana M. Mancho. 2015. "Lagrangian Descriptors for Two Dimensional, Area Preserving, Autonomous and Nonautonomous Maps." *Communications in Nonlinear Science and Numerical Simulation* 27 (1-3): 40–51.

Madrid, J. A. J., and A. M. Mancho. 2009. "Distinguished trajectories in time dependent vector fields." *Chaos* 19: 013111.

Mancho, A. M., S. Wiggins, J. Curbelo, and C. Mendoza. 2013. "Lagrangian Descriptors: A Method for Revealing Phase Space Structures of General Time Dependent Dynamical Systems." *Communications in

Nonlinear Science and Numerical 18: 3530–57.

Mendoza, C., and A. M. Mancho. 2010. "The hidden geometry of ocean flows." *Phys. Rev. Lett.* 105 (3): 038501.

Mendoza, C., A. M. Mancho, and S Wiggins. 2014. "Lagrangian Descriptors and the Assessment of the Predictive Capacity of Oceanic Data Sets." *Nonlinear Processes in Geophysics* 21 (3). Copernicus GmbH: 677–89.

Oliveira, H. P. de, A. M. Ozorio de Almeida, I. Damião Soares, and E. V. Tonini. 2002. "Homoclinic chaos in the dynamics of a general Bianchi type-IX model." *Phys. Rev. D* 65 (8): 9.

Patra, Sarbani, and Srihari Keshavamurthy. 2018. "Detecting Reactive Islands Using Lagrangian Descriptors and the Relevance to Transition Path Sampling." *Physical Chemistry Chemical Physics* 20 (7). Royal Society of Chemistry: 4970–81.

Ramos, A. G., V. J. García-Garrido, A. M. Mancho, S. Wiggins, J. Coca, S. Glenn, O. Schofield, et al. 2018. "Lagrangian Coherent Structure Assisted Path Planning for Transoceanic Autonomous Underwater Vehicle Missions." *Scientfic Reports* 4: 4575.

Revuelta, F, Galen T Craven, Thomas Bartsch, F Borondo, RM Benito, and Rigoberto Hernandez. 2017. "Transition State Theory for Activated Systems with Driven Anharmonic Barriers." *The Journal of Chemical Physics* 147 (7). AIP Publishing: 074104.

Waalkens, H., and S. Wiggins. 2004. "Direct Construction of a Dividing Surface of Minimal Flux for Multi-Degree-of-Freedom Systems That Cannot Be Recrossed." *Journal of Physics A: Mathematical and General* 37 (35). IOP Publishing: L435.

———. 2010. "Geometrical Models of Phase Space Structures Governing Reaction Dynamics." *Regular and Chaotic Dynamics* 15 (1): 1–39.

Waalkens, H., R. Schubert, and S. Wiggins. 2008. "Wigner's Dynamical Transition State Theory in Phase Space: Classical and Quantum." *Nonlinearity* 21: R1–R118.

Wiggins, S. 1990. "On the Geometry of Transport in Phase Space I. Transport in k Degree-of-Freedom Hamiltonian Systems, $2 \leq k < \infty$." *Physica D* 44: 471–501.

———. 2013. *Normally Hyperbolic Invariant Manifolds in Dynamical Systems*. Vol. 105. Springer Science & Business Media.

———. 2016. "The Role of Normally Hyperbolic Invariant Manifolds (Nhims) in the Context of the Phase Space Setting for Chemical Reaction Dynamics." *Regular and Chaotic Dynamics* 21 (6): 621–38.

Wigner, Eugene. 1938. "The Transition State Method." *Transactions of the Faraday Society* 34 (0). The Royal Society of Chemistry: 29–41.